energies

MDPI

Review

Advances in Modeling and Optimization of Intelligent Power Systems Integrating Renewable Energy in the Industrial Sector: A Multi-Perspective Review

Lei Zhang [1,2], Yuxing Yuan [1,2], Su Yan [1,2], Hang Cao [1,2] and Tao Du [1,2,*]

[1] Key Laboratory of Eco-Industry, Ministry of Ecology and Environment, Northeastern University, Shenyang 110819, China
[2] Engineering Research Center of Frontier Technologies for Low-Carbon Steelmaking, Ministry of Education, Shenyang 110819, China
* Correspondence: dut@mail.neu.edu.cn

Abstract: With the increasing liberalization of energy markets, the penetration of renewable clean energy sources, such as photovoltaics and wind power, has gradually increased, providing more sustainable energy solutions for energy-intensive industrial sectors or parks, such as iron and steel production. However, the issues of the intermittency and volatility of renewable energy have become increasingly evident in practical applications, and the economic performance and operational efficiency of localized microgrid systems also demand thorough consideration, posing significant challenges to the decision and management of power system operation. A smart microgrid can effectively enhance the flexibility, reliability, and resilience of the grid, through the frequent interaction of generation–grid–load. Therefore, this paper will provide a comprehensive summary of existing knowledge and a review of the research progress on the methodologies and strategies of modeling technologies for intelligent power systems integrating renewable energy in industrial production.

Keywords: smart microgrid; renewable energy; modeling techniques of prediction; modeling techniques for microgrid scheduling

check for updates

Academic Editor: Angela Russo

Received: 3 April 2025
Revised: 28 April 2025
Accepted: 9 May 2025
Published: 11 May 2025

Citation: Zhang, L.; Yuan, Y.; Yan, S.; Cao, H.; Du, T. Advances in Modeling and Optimization of Intelligent Power Systems Integrating Renewable Energy in the Industrial Sector: A Multi-Perspective Review. *Energies* **2025**, *18*, 2465. https://doi.org/10.3390/en18102465

Copyright: © 2025 by the authors. Licensee MDPI, Basel, Switzerland. This article is an open access article distributed under the terms and conditions of the Creative Commons Attribution (CC BY) license (https://creativecommons.org/licenses/by/4.0/).

1. Introduction

Under the multiple pressures from capacity reduction, financial performance, and carbon control requirements, the industrial sectors are facing unprecedented challenges in energy conservation and low-carbon transition [1,2]. The industrial enterprises generally encounter the following issues in electricity utilization: high indirect emissions due to a heavy reliance on coal-fired power, high external electricity costs with considerable susceptibility to price fluctuations, insufficient energy management and low power conversion efficiency, and significant electricity load fluctuations and low effectiveness of power matching. The Paris Agreement [3] emphasizes the importance of accelerating the energy transition and expediting the deployment of renewable energy. Although enhancing electricity conservation is essential in the typical industrial production processes [4], the rapid advancements in renewable energy technologies have led to growing attention on integrating variable renewable energy sources into power grids and improving their penetration to mitigate electricity-induced carbon emissions [5,6].

With the growing penetration of renewable energy, traditional power systems are experiencing heightened complexity. If not carefully designed, the integration of microgrids with conventional power systems may lead to issues such as degraded power quality,

reduced reliability, instability, and security concerns [7]. Power systems are prioritizing the flexible management of variable renewable energy sources. By incorporating distributed generation, energy storage, and advanced smart technologies, modern microgrids establish novel electricity-utilization frameworks and solutions, offering significant potential for future development [8]. The construction of smart microgrids holds significant importance in the following aspects [9–12]: enhancing the local production and consumption of renewable energy; facilitating the complementary use of multiple energy sources; improving the resilience and reliability effectively; increasing the operational flexibility; enhancing the economics of power grids, and promoting environmental sustainability.

The development and application of industrial microgrids are still in their initial stages, but some related research has already been conducted in this field. Blake et al. [13] utilized historical data to generate facility load forecasts and conducted a scenario analysis to examine the impact of the distributed energy operation and demand response on carbon emissions and energy costs in industrial microgrids. Li et al. [14] designed an operational framework for an industrial microgrid powered by wind energy and developed a multi-objective optimization model with a comprehensive consideration of operational costs and user satisfaction. Misaghian et al. [15] presented a new framework for the optimal operation of industrial microgrids, which consists of three levels, each designed to address different issues. Guo et al. [16] established a novel industrial microgrid architecture to optimize the operation of the power grid using the flexible potential of responsive electric vehicles and developed a scheduling model to minimize the operational costs of industrial microgrids. Daneshvar et al. [17] proposed a novel techno-economic risk-mitigation strategy for the optimal scheduling of industrial microgrids, considering both technical and economic objectives.

In addition, several industrial microgrid projects have been unveiled as benchmark demonstrations. The Philadelphia Navy Yard in the United States underwent an upgrade in 2014, constructing an advanced power distribution system and reliable electricity [18]. The shipyard has been established as a national hub for emerging smart grid practices. The microgrid of Xi'an Industrial Park in China can achieve a two-stage demand response based on the capacity electricity price, which includes the world's first high-voltage, grid-connected PV power station, 1-MW/1-MWh lithium battery energy storage system, and a 960 kW charging station [19]. The TUPRAS facility located in the north-western region of Turkey designed a successful microgrid structure, which proved effective during severe grid faults including blackouts [20]. In 2023, BYD's photovoltaic and energy storage project located in Chongqing successfully achieved full-capacity operation. This project achieved the integrated applications of rooftop photovoltaic power generation, electrochemical energy storage, and production line energy recovery. Additionally, the alteration of key equipment was carried out, replacing traditional AC/DC power supplies with DC to power the charging stations.

The main contributions of this work are as follows:

- The widespread adoption and development of industrial microgrids remain in the exploratory stage, without comprehensive standardized frameworks for their fundamental architecture and operational patterns. This review describes the fundamental architecture, configuration, and operational characteristics of industrial microgrids, providing theoretical support for their programming and application.
- The volatility and complexity of renewable energy and industrial loads restrict the accuracy and adaptability of traditional source-load forecasting methods, hurting microgrids' economical and reasonable scheduling. This review examines multiple intelligent modeling strategies for source-load forecasting to provide a range of alternatives for increasing the quality of microgrid scheduling decisions.
- The existing microgrid scheduling optimization methods exhibit distinct advantages and disadvantages, making them inadequate for the efficient operation of complex

industrial scenarios. This review summarizes general modeling approaches for industrial microgrid scheduling, laying the foundation for the intelligent management of industrial microgrids.

2. Review Methodology and Strategy

2.1. Scope of Literature Search

Defining the scope of the literature search is critical to ensuring that the research is scientifically rigorous. This review primarily aims to assess the fundamental knowledge, theoretical frameworks, and significant progress in the microgrid and its modeling techniques, thereby identifying potential challenges and future development directions. Research articles, conference papers, reviews, and reports are included in the selected literature examined in this review. Every effort was made to incorporate the most recent research conducted during the previous five years to ensure that the analysis reflects the latest advancements in this field. The literature search was conducted across a diverse set of highly reputable databases, including Web of Science, Google Scholar, MDPI, IEEE Xplore, Springer, ScienceDirect, Scopus, ResearchGate, and CNKI, using keywords such as "microgrid", "demand response", and "renewable energy". Furthermore, the search was restricted exclusively to publications in English to maintain consistency across different sources.

2.2. Criteria of Literature Selection

In addition to establishing a rigorous scope, well-defined exclusion criteria should be incorporated during the review process to select highly relevant literature. During the initial screening phase, particular attention should be given to whether the article titles and keywords align with the core topics of microgrids and their modeling techniques, while promptly discarding studies with low relevance or those that deviate from the research direction. We employed VOSviewer 1.6.20 to conduct a bibliometric analysis of the relevant literature in this field and summarized the main keywords related to microgrid modeling research, as shown in Figure 1. Subsequently, a detailed investigation of the abstracts is necessary to further ensure the relevance to the field, as well as to evaluate the depth of analysis and the degree of innovation. In addition, special attention should be paid to studies that demonstrate significant breakthroughs in research methods and conclusions.

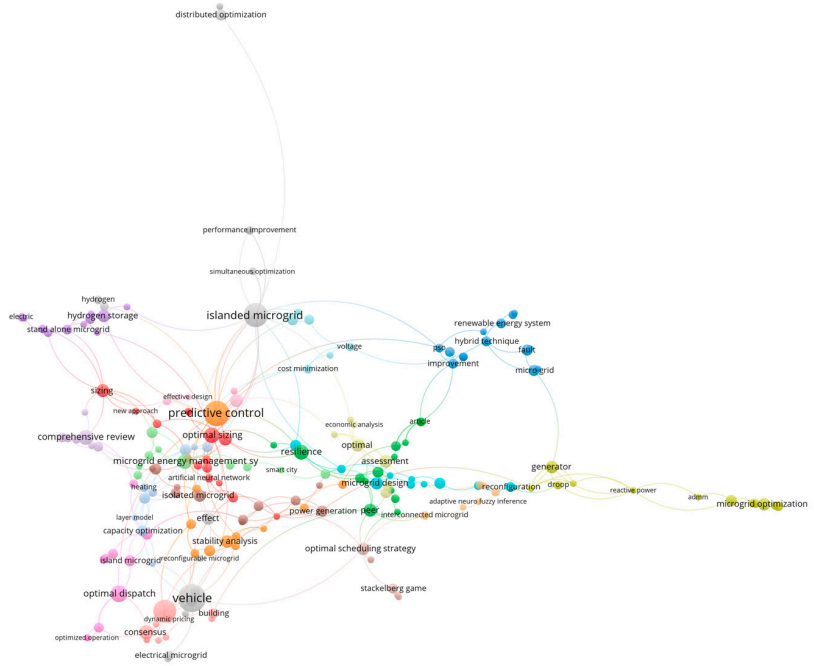

Figure 1. Main keywords in the field of microgrid modeling research.

2.3. Review Methodology

A comprehensive and critical review was conducted by employing methodologies such as classification and a comparative analysis. The reviewed studies were subjected to thematic extraction and key point summarization, categorized and organized according to distinct research perspectives and methodologies, thereby constructing a hierarchical knowledge framework. Furthermore, a detailed comparative analysis and feature-based evaluation of different methods, technologies, and structural components were performed to identify the underlying characteristics and key distinctions.

3. Basic Concept and System Architecture of Smart Microgrid

3.1. Fundamental Concepts and Response Functions of Smart Microgrids

3.1.1. Smart Microgrid

The energy utilization in industrial sectors is currently challenged by multiple factors, including rising operational costs, energy efficiency limitations [21], and the increasing environmental impact [22]. The growing demand for electricity, coupled with the continued reliance on traditional technological solutions, is exacerbating the complexity of power networks and highlighting their lack of long-term sustainability [23]. Achieving the effective integration of conventional and renewable energy sources, along with the implementation of intelligent energy management strategies [24,25], presents promising opportunities to address these challenges. Microgrids [26,27], advanced power networks with complex autonomous operational capabilities, are composed of distributed power sources, energy storage devices, and loads arranged according to a specific topological structure, with intelligence constituting a crucial attribute of smart microgrids [28]. The comparison between traditional power grids and microgrids is shown in Table 1. Microgrids are small-scale distribution systems that effectively integrate renewable and conventional distributed energy sources into the power subsystem, characterized by multi-source low-inertia power supply, multi-mode coordinated operation, multi-module complementary support, and flexible interaction within a multi-level architecture [29]. Microgrids can function in conjunction with the public grid (grid-connected mode) or independently of the public grid during faults or external disturbances (islanded mode), which is one of their primary capabilities and distinguishing features [30]. Kakran et al. [31] define microgrids as a technology that maximizes the benefits for utilities and their consumers and provides economical and reliable power services by effectively utilizing available resources and intelligent tools. In addition to the energy flow, smart microgrids integrate larger-scale information flow compared to traditional power grids [32], which collect and transmit various types of real-time data, including the equipment status, power load, and user interaction data. Subsequently, smart microgrids can accurately forecast power supply and demand and optimize operational performance by employing advanced data analysis techniques [33]. Data-driven approaches provide comprehensive decision support for the efficient operation of smart microgrids, as illustrated in Figure 2 [34].

Table 1. Comparison between a traditional grid and smart microgrid.

Characteristics	Conventional Grid	Smart Microgrid
Scale and scope	Wide coverage range	Small coverage area
Power resources	Single traditional thermal power	Abundant renewable energy
Control method	Centralized control	Diverse control methods
Flexibility	Limited	High
Response speed	Hysteretic response	Rapid response
Security	Insufficient	Relatively stronger resilience
Informatization	Limited informatization	Strong information exchange capability
Economics	Dependent on electricity price	Lower operational cost
Environmental impact	Higher greenhouse gas emissions	Lower greenhouse gas emissions
Efficiency	The l energy efficiency of combined heat and power (CHP) systems can reach 75% to 80%	The overall energy efficiency can reach 85% to 95%

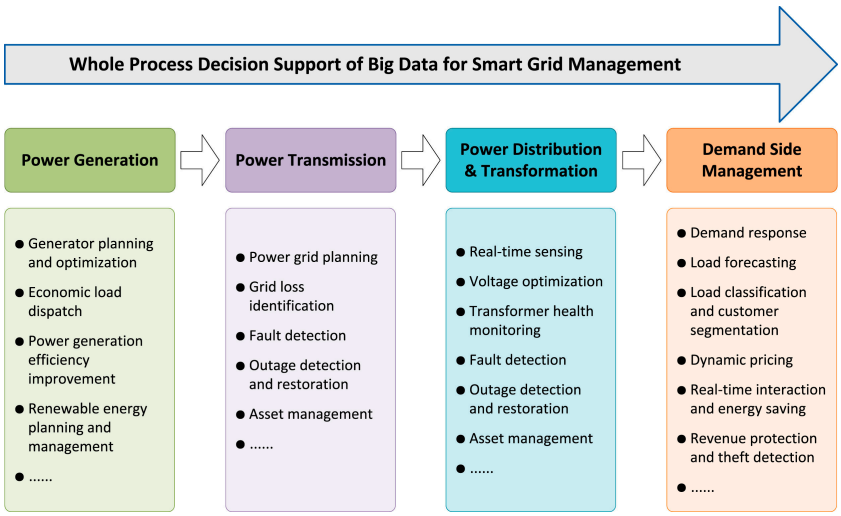

Figure 2. Whole process decision support of big data for smart microgrid management [34].

3.1.2. Demand-Side Flexibility

Demand-side flexibility (DSF) refers to the ability of electricity consumers to adjust their power-consumption behavior based on demand, primarily implemented through demand response (DR) measures. The demand response generally refers to the short-term adjustments in electricity-utilization strategies by users in response to price signals or incentives, particularly during significant fluctuations in prices of electricity or threats to system security and reliability. In addition, demand response strategies also include hybrid approaches based on both price signals and incentives, demand response exchange, load shifting, and others [35]. In the early stages, demand-side management primarily relied on mandatory load control to mitigate electricity overload and peak load pressures. However, with the progressive development of electricity markets, demand-side management has transitioned from compulsory interventions to market-oriented regulation. An active demand response [36,37] relies on advanced information and communication technologies to guide users in autonomously adjusting their electricity-consumption behavior through price signals or incentive mechanisms, thereby achieving more flexible and efficient power load regulation. The incentive-based demand response [38] motivates users to adjust their electricity load during peak periods by offering economic incentives and compensation. Operators establish contracts with users in advance, and the users reduce or interrupt part of their load during specified periods to receive corresponding compensation, thereby mitigating supply–demand imbalances through load-side participation in scheduling. In price-based demand response programs, consumers adjust their electricity-consumption behavior in response to price fluctuations, including time-of-use pricing and real-time pricing [31].

3.2. System Architecture of Microgrid

3.2.1. Basic Architecture of Microgrid

The basic architecture of a smart microgrid can primarily be divided into four layers: the physical component layer, the communication layer, the control layer [39], and the business layer [40]. The physical component layer consists of distributed micro power sources, loads, energy storage devices, power converters, and common coupling points, forming the infrastructure of the smart microgrid, involving the production, storage, conversion, and consumption of electricity. The communication layer interfaces with other layers through networks and protocols to facilitate information sharing and data exchange. The control layer manages the operating status of physical components based

on the collected data, enabling real-time power scheduling and management. The business layer is responsible for the flexible development of business models.

(1) Physical component layer

Distributed energy sources encompass both traditional and renewable power generation. Thermal power units and cogeneration are traditional ways of power generation, whereas photovoltaic, wind power, biomass power, and hydrogen fuel cells [41–45] are examples of renewable energy generation. The power system's loads can be classified into controllable and uncontrollable types [29]. Uncontrollable loads demand high supply stability and cannot be readily adjusted or interrupted. In contrast, controllable loads are flexible and can be regulated according to operational requirements. Moreover, the microgrids balance the power supply and demand by using energy storage devices and various control strategies [46], mitigating fluctuations in renewable energy output and compensating for the variability and intermittency of distributed power sources. Energy storage systems charge during low-load periods and discharge during peak-load periods, serving as an energy buffer to achieve peak shaving and valley filling, while smoothing voltage fluctuations in the grids. The typical energy storage technologies can be divided into five categories: mechanical energy storage systems (MESSs), electric energy storage systems (EESSs), electrochemical energy storage systems (ECESSs), thermal energy storage systems (TESSs), and chemical energy storage systems (CESSs), which have been detailed in Table A1 [47].

(2) Communication layer

The current communication infrastructure of traditional power grids generally supports only unidirectional power flow from power plants to consumers, resulting in limited efficiency and capability of information sharing [48]. Transforming traditional microgrids into smart microgrids requires the deployment of more powerful, economical, efficient, and appropriate communication infrastructure to support the handling of vast data flows and bidirectional communication capabilities [49]. The capability to collect data and communicate with various devices in the power grid is revolutionizing the operational practices of utility companies [50,51]. Smart microgrids can be regarded as typical cyber–physical systems, with their communication layer employing various protocols, such as Modbus, DNP3, IEC 61850, MQTT, and OPC UA, to ensure device compatibility and efficient data transmission. Typical communication frameworks involve master–slave, publish–subscribe, and client–server architectures. In addition, communication networks can generally be set up in different ways, including wide area networks (WANs), metropolitan area networks (MANs), local area networks (LANs), and personal area networks (PANs) [52].

(3) Control layer

The operational microgrids face multiple challenges, such as bidirectional power flow, local oscillation and stability, low inertia, and uncertainty issues. Advanced protection and control systems are required to mitigate these impacts and ensure the reliable and economical operation of microgrids [53]. The control architecture of microgrids mainly consist of centralized, decentralized, and distributed control, along with hierarchical control schemes at the primary, secondary, and tertiary levels, which represent a compromise between fully centralized and fully decentralized approaches [54]. Considering the functionality of distributed generation within microgrids, the control methods can also be classified into master–slave, hierarchical, or peer-to-peer type. Modu et al. [55] divided the control architecture of DC microgrids into basic control strategies and hierarchical control structures, as shown in Figure 3.

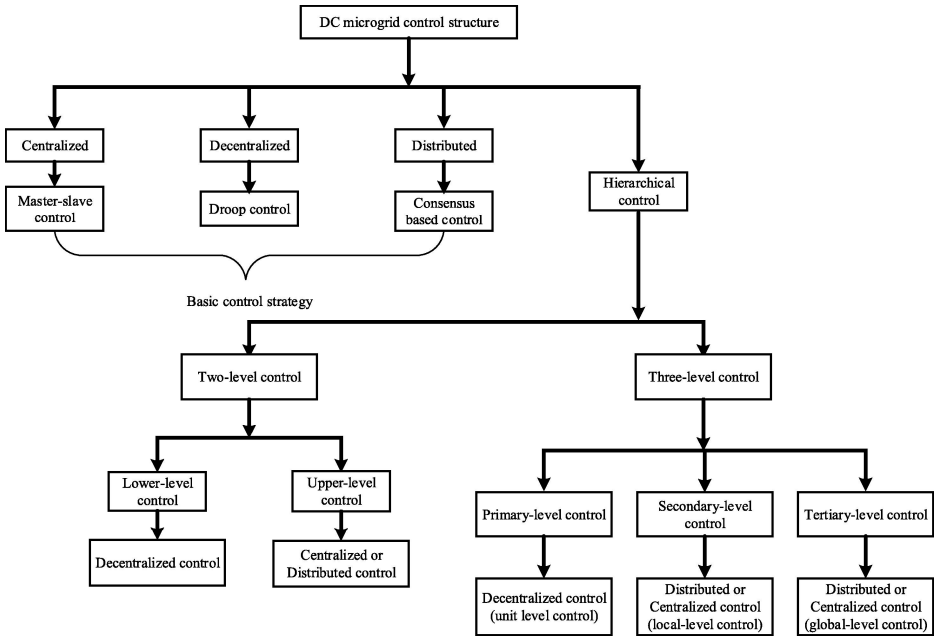

Figure 3. Basic control strategies and structures for microgrids [55].

3.2.2. Power Supply Modes of Microgrids

Initially, DC grids were widely used for the power supply, but inefficiencies arose due to the unresolved issues of power loss and voltage drops. The appearance of transformers and AC technology facilitated the widespread adoption of AC power systems [56,57]. Nevertheless, as DC sources and loads continue to penetrate the power grid, DC grids are gradually becoming an essential component of future power systems [58]. Currently, the microgrids can be classified into three main categories, depending on the way in which the AC and DC buses are connected [30]. AC microgrids achieve the interconnection of physical components via a shared AC bus. In DC microgrids, the DC bus is connected to the grid through an AC/DC converter, enabling direct connection to the DC bus with a single power conversion. Hybrid AC/DC microgrids integrate both AC and DC buses simultaneously. The characteristics of different microgrid connection methods are shown in Table 2.

Table 2. Characteristics of different bus connection methods [59].

Characteristics	DC Microgrid	AC Microgrid
Number of converters	Medium	High
Transmission efficiency	High; no loss associated with the reactive power	Low; the reactive power increases the transmission losses
Stability margin	High	Low
Power supply reliability	High reliability with smooth transient	A seamless transition is challenging to ensure after a grid fault
Control	Simple	Complex but relatively mature
Load compatibility	More compatible with distributed power sources	More compatible with traditional AC power grid
Protection system	Complex and costly	Simple and affordable
Devices compatibility	No	Yes
Skin effect	Not existed	Yes

3.2.3. Flexible Microgrids Integrating Industrial Loads

Electrification is regarded as an important decarbonization option for the industrial sector, with the most direct approach being the replacement of power loads in industrial

process with zero-carbon power sources [60]. For example, the use of zero-carbon electricity could decarbonize up to 13.3% of the iron- and steel-production process. In terms of the iron and steel industry, facilitating the transition from the traditional BF-BOF process to the DRI-EAF process would further enhance the decarbonization potential based on zero-carbon electricity [61]. Some of the key objectives of iron and steel plants are to improve energy efficiency, reduce carbon emissions, and lower energy production costs [62,63]. The widespread deployment of renewable energy in industrial parks, coupled with the volatility of both intermittent and continuous loads in the iron and steel industry [64], makes the effective management of both the supply side and the demand side essential [65].

The industrial manufacturing process can be classified into continuous and non-continuous processes, with each type necessitating differentiated demand response strategies. For continuous production industries, such as the iron and steel industry, flexibility is typically achieved through load shifting and reduction. The non-continuous industries offer greater flexibility in choosing adjustment methods. In addition, load regulation in industrial sites can be achieved by modifying the production temperature, production speed, input current, or voltage. The iron and steel industry typically adjusts loads through temperature control, such as modifying the high-temperature refining time and heating rate of refining furnaces. The electrolytic aluminum industry typically regulates loads by adjusting the current and voltage [66].

The possible low-carbon microgrid based on iron and steel production is shown in Figure 4. By-product gases generated during the coking, ironmaking, and steelmaking processes are transported to the captive power plant for combustion-based power generation to meet the electricity demands of industrial production. The uncertainty of by-product gas is also a significant factor affecting power stability, thereby necessitating the targeted development of a gas scheduling system [67–69]. Meanwhile, waste heat and residual energy [70,71] are recovered and used by equipment, such as an annular cooler, dry coke quenching, top-pressure recovery turbines (TRTs), and evaporation cooling for power generation, as an additional power source. Furthermore, photovoltaic (PV), wind energy, hydrogen, and energy storage systems are deployed within the industrial power system to reduce the proportion of purchased electricity in the overall power structure.

The cost of electricity in aluminum electrolysis plants can account for 30% to 40% of the total production cost [72], making it economically significant to adopt lower-cost power sources. Power plants supply electricity directly to aluminum production loads, while the public grid is used to compensate for the power imbalance between generation and load. The electrolytic aluminum load functions as a thermal storage load, with short-term adjustments having minimal impact on production. The power can be regulated within a 25% range, and continuous operation for up to 4 h will not cause coagulation in the electrolytic cell. The primary production process involves transferring a 160 kA direct current into an electrolytic cell containing bauxite, cryolite, and catalysts, where aluminum oxide is reduced to molten aluminum at temperatures between 950 and 970 °C [73]. Sgouris et al. [74] operated an aluminum smelting plant using 100% renewable energy by installing single-axis tracking photovoltaics, wind power, battery storage, and hydrogen storage, as shown in Figure 5.

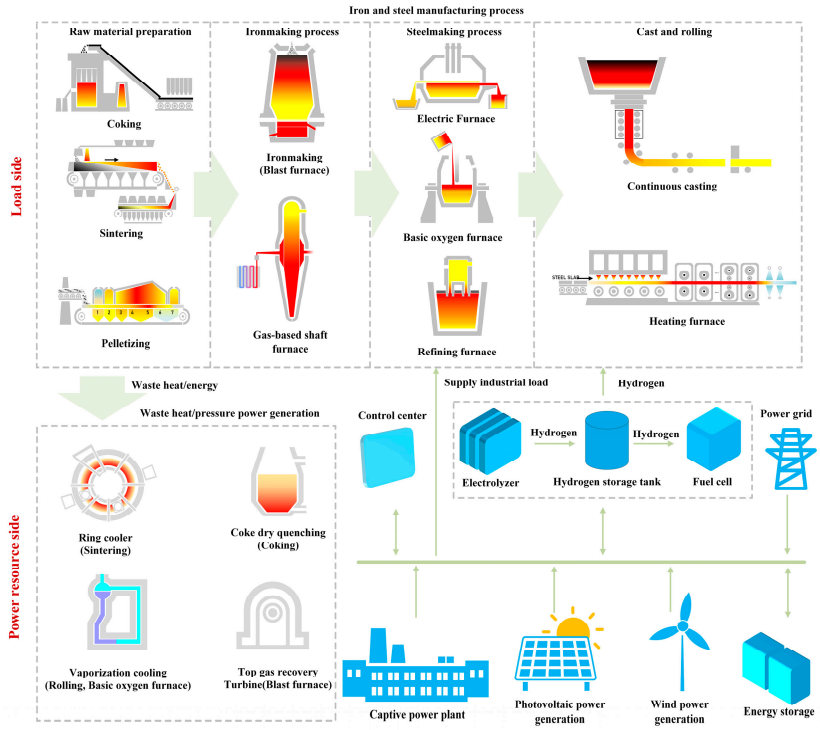

Figure 4. System architecture of smart microgrid integrated with renewable energy and industrial loads in iron and steel production sector. In the diagram of the pelletizing process, sections numbered 1 to 7 correspond to different zones based on airflow distribution and functional differentiation: the blast drying zone, the draft drying zone, the preheating zone, the roasting zone, the soaking zone, the first cooling zone, and the second cooling zone.

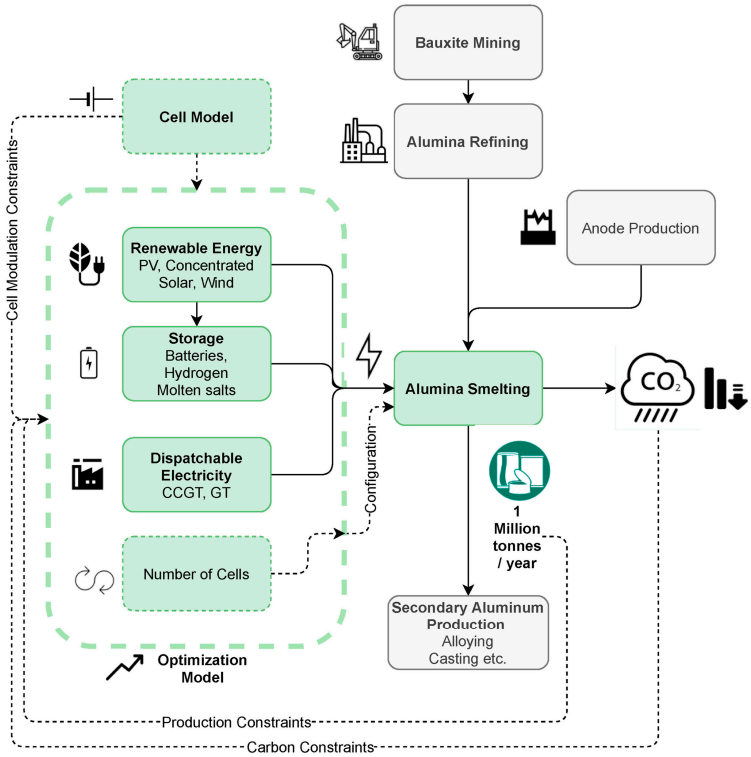

Figure 5. Aluminum smelter configuration integrated with renewable energy [74].

4. Modeling Technologies for Intelligent Prediction

Achieving more accurate predictions of power sources and loads in industrial processes can reduce operational risks, facilitate the rational planning of electricity use, and enhance the stability and reliability of the power network [75]. Traditional forecasting methods primarily include physical models and statistical models. The physical models simulate the operation of a power system based on established rules and mechanisms. Statistical models achieve forecasting by correlating historical values with predicted values based on historical data patterns, which often leverage prior knowledge and assumptions to reduce model complexity, including methods such as regression analysis, time series analysis, and exponential smoothing. The regression method predicts the possible values of the dependent variables by establishing a mathematical relationship model between the independent and dependent variables. The time series method constructs a mathematical model by fitting curves and estimating parameters based on historical data. This method assigns different weights to historical data from different periods and predicts data through exponentially weighted combinations [76]. Conventional load forecasting methods are characterized by low model complexity and high interpretability; however, they exhibit relatively low predictive accuracy and weak generalization capability, posing inherent limitations in managing complex nonlinear relationships and high-dimensional data [77]. Consequently, prediction methods based on artificial intelligence models (machine learning) [78,79] have gained growing interest, with the forecasting procedure primarily including data processing, forecasting strategies selection, prediction through modeling, and model evaluation.

4.1. Raw Data Processing

Microgrid systems are usually equipped with data acquisition and monitoring systems, such as SCADA systems and IoT sensors, which enable real-time and accurate data collection, thereby supporting efficient decision-making processes. SCADA systems can be used for real-time monitoring, control, and data acquisition in microgrids, consisting of a combination of sensors, smart meters, field devices, RTUs, PLCs, and other various software or hardware components. The IoT sensors are information-acquisition devices within the architecture of the Internet of Things (IoT), primarily designed to collect data and transmit it from the physical environment to digital networks. The collected raw data frequently exhibit incompleteness, noise, and inconsistency, resulting in poor data quality and substantially reducing the predictive accuracy. Therefore, preprocessing techniques, including classification, clustering, and association, must be employed to improve data quality [80,81]. Fan [82] outlined the primary tasks and common methods in data preprocessing, encompassing data cleansing, data reduction, data augmentation, data transformation, and data partitioning, as illustrated in Figure 6. This section provides a detailed review of data cleaning and reduction technologies.

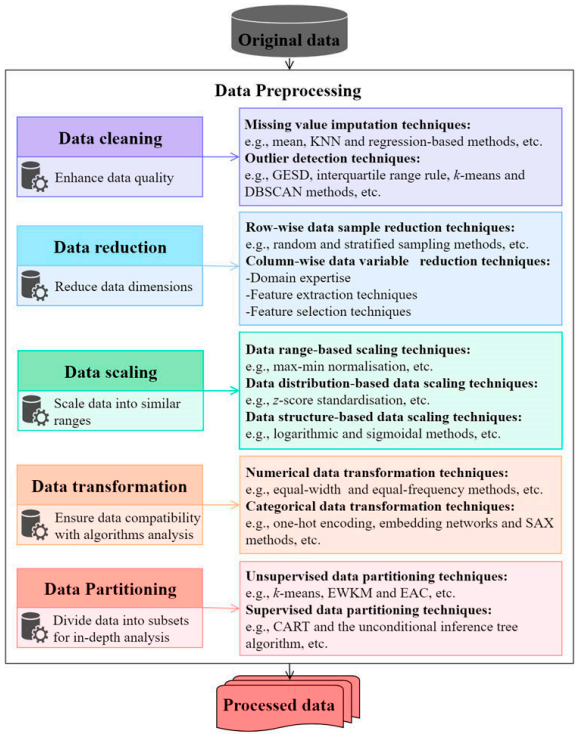

Figure 6. Typical data preprocessing tasks for building operational data analysis [82].

4.1.1. Data Cleaning

Data cleaning aims to remove irrelevant and duplicate information, correct outliers, fill in missing values, and ensure consistency in data formatting. Hosseinzadeh et al. [83] classified data cleaning mechanisms into five categories based on execution methods: machine-learning-based, sample-based, expert-based, rule-based, and framework-based approaches.

The elimination of duplicate data is a key task of identifying redundant records to enhance data quality, and the existing deduplication methods in the Industrial Internet of Things environment frequently face challenges in terms of efficiency and scalability [84]. Altowaijriet et al. [84] emphasized the necessity of developing an efficient data aggregation scheme based on grid hashing.

Anomaly detection aims to identify and handle outliers or anomalies that deviate from the overall data distribution; nevertheless, not all detected anomalies necessarily need to be removed or replaced [85]. Numerous anomaly detection methods based on machine learning have been proposed [86], including unsupervised detection (clustering, one-class learning, dimensionality reduction), supervised detection (deep learning, classical neural networks, regression, probabilistic models, conventional algorithms), ensemble learning (boosting, bagging), feature extraction (distance-based, density-based, time series), and hybrid learning [87]. For example, Chen et al. [88] proposed an adaptive outlier-based non-crossing quantile regression model for day-ahead electricity price forecasting, aiming to improve the reliability and clarity of the forecasting interval. Liang et al. [89] developed an outlier-detection model for big data of power based on the fuzzy K-means clustering algorithm, which significantly improves the complexity, accuracy, and efficiency of outlier detection by optimizing the initial clustering centers. Oza [90] proposed a novel one-class classification method based on convolutional neural networks. Zhang et al. [91] proposed an adaptive anomaly-detection method based on particle swarm optimization (PSO) and support vector machines (SVM) for detecting abnormal power consumption using time series data in advanced metering infrastructure.

Missing value imputation aims to estimate and fill in missing values within a dataset to improve data integrity and prediction accuracy. The imputation processes typically follow two strategies [92]: if the missing rate is less than 10% or 15%, the missing data can simply be discarded without significantly affecting the final analysis results; if the missing rate exceeds 15%, the employment of imputation methods is necessary [93]. Considering data uncertainty, imputation methods can be categorized into single imputation and multiple imputation [94]. In addition, depending on whether they are inspired by machine learning, imputation methods can be classified into statistical-based methods and machine learning-based methods [95,96]. Statistical-based imputation techniques, inspired by traditional statistical process models and procedures, offer strong interpretability and computational efficiency in handling data integrity, including the mean, mode, expectation, linear regression, and least squares. Machine-learning-based imputation techniques leverage the internal structure and feature correlation of data, with clustering, decision trees, K-nearest neighbors, and random forests being the most commonly used methods [93]. When selecting specific imputation techniques, the missing data mechanism, the missing pattern, and missing rate should be fully considered [97]. Bülte et al. [98] developed a two-step method based on an attention model to estimate missing values in multivariate time series. Zheng et al. [99] introduced a hybrid factor analysis for estimating missing values in the dataset of power load, developed a screening process to identify anomalies in electricity data, and applied multiple imputation techniques using chained equation-based linear regression to impute missing values and replace anomalies [100].

4.1.2. Data Reduction

The main purpose of data reduction is to condense the original dataset, obtaining a reduced dataset that retains the integrity of the original data [101]. Feature engineering [102] simplifies data by converting or removing high-dimensional features into low-dimensional features, which reduces data complexity, improves model performance, and strengthens the generalization capability [103].

Feature selection reduces data dimensionality by filtering or removing low-correlation or irrelevant features. The related methods can be categorized based on evaluation criteria into filter methods, wrapper methods, and embedded methods or into exhaustive search algorithms, heuristic search algorithms, and random search algorithms according to search strategies [104–106]. Filter methods (Pearson coefficient, chi-square test, mutual information, Euclidean distance, variance test, etc.) independently assess the correlation of individual features according to specific criteria without considering feature interactions, offering the advantage of high speed without requiring classification algorithms [107]. Wrapper methods (forward selection, backward search, recursive feature elimination, etc.) evaluate feature subsets based on the performance of learning algorithms, enabling the full consideration of feature interactions. Embedded methods (regularization-based methods, tree-based methods, etc.) incorporate feature selection into the model-construction process, optimizing the feature subset simultaneously with model training [108]. Liu et al. [109] highlighted the critical role of feature selection in energy consumption forecasting and identified three highly relevant feature categories: historical load data, weather information, and timestamp features. Salcedo et al. [110] introduced a wrapper-based feature selection method based on a novel meta-heuristic approach for feature selection in renewable energy data. Amer et al. [111] applied the Pearson correlation coefficient to pinpoint critical weather variables influencing the output of a power plant.

Feature extraction transforms high-dimensional data into low-dimensional data with more concentrated information by mapping the original data into a new feature space, aiming to improve model performance while retaining key information. The extraction

algorithms can be classified into two types: linear methods, which were initially used for dimensionality reduction due to their computational simplicity, and nonlinear methods, which have gained more attention with the growing complexity of nonlinear and time-varying systems and scenarios. Representative linear feature extraction methods include principal component analysis (PCA), linear discriminant analysis (LDA), factor analysis (FA), independent component analysis (ICA), multidimensional scaling (MDS), and singular value decomposition (SVD) [105], while nonlinear feature extraction methods mainly focus on kernel-based optimization, non-negative matrix factorization (NMF), and information-theoretic approaches.

4.2. Prediction Strategy Selection

The forms of prediction can be classified into one-step prediction and rolling prediction. One-step prediction refers to forecasting multi-step in advance, where the output test set includes all desired prediction points. Rolling prediction generates sequential outputs, where each step's output serves as part of the next input, continuously updating the prediction results.

Predictions can also be categorized into four types based on the time scale and timeliness: ultra-short-term, short-term, medium-term, and long-term predictions. Ultra-short-term prediction (less than 60 min) is typically used for real-time power dispatch and a rapid response. Short-term prediction (within the range of 1 h to 7 days) is usually applied to forecast the previous day's and medium-term's trends, such as day-ahead market trading and day-ahead load scheduling. Medium-term prediction (within the range of 7 days to 30 days) is generally used for the architecture and maintenance of the power system or the power trading planning. Long-term prediction (from 30 days to 1 year) is typically employed for the operational and planning design of a power system [112–114].

Additionally, forecasts can be divided into deterministic and uncertain forecasting based on the form of the forecasting results. Point forecasting refers to a deterministic forecast that offers a precise value at a specific time and its associated error, which can contribute to the formulation of concrete scheduling plans in industrial power systems [115]. Uncertainty forecasting [116] encompasses interval forecasting and probabilistic forecasting. Interval forecasting provides the fluctuation range of the forecasted object, while the probabilistic forecasting provides the cumulative distribution function or probability density function of the forecasted object, characterizing the possibility of the forecasted object within a defined range. Based on data-driven and deep learning methods, Niu et al. [117] proposed a hybrid ultra-short-term power forecasting framework capable of achieving accurate point-to-point wind power forecasting using the time series data of wind power, resulting in more reliable interval predictions. Zhang et al. [118] combined artificial intelligence methods with statistical knowledge to propose a wind speed interval forecasting model based on weather data. Chang et al. [119] developed a two-stage probabilistic load forecasting framework that integrates point forecasts as essential probabilistic forecasting features. To address the limitations of traditional scheduling strategies, which tend to ignore the deterioration of forecasting accuracy over time and lack a mechanism for defining optimal forecasting ranges, Diego Aguilar et al. [120] integrated machine-learning-based probabilistic forecasting with robust optimization to formulate an optimal scheduling plan for the microgrid.

4.3. Prediction Model

Several commonly used machine learning algorithms applicable to energy system modeling and forecasting are shown in Figure 7, including supervised learning, unsupervised learning, semi-supervised learning, and reinforcement learning. Deep learning

focuses on feature learning based on multi-layer neural networks and has evolved into an independent branch of machine learning. The aforementioned algorithms can be flexibly applied to tasks such as load forecasting and output forecasting, depending on the specific characteristics and modeling requirements of energy systems. The basic process of machine learning methods is illustrated in Figure 8.

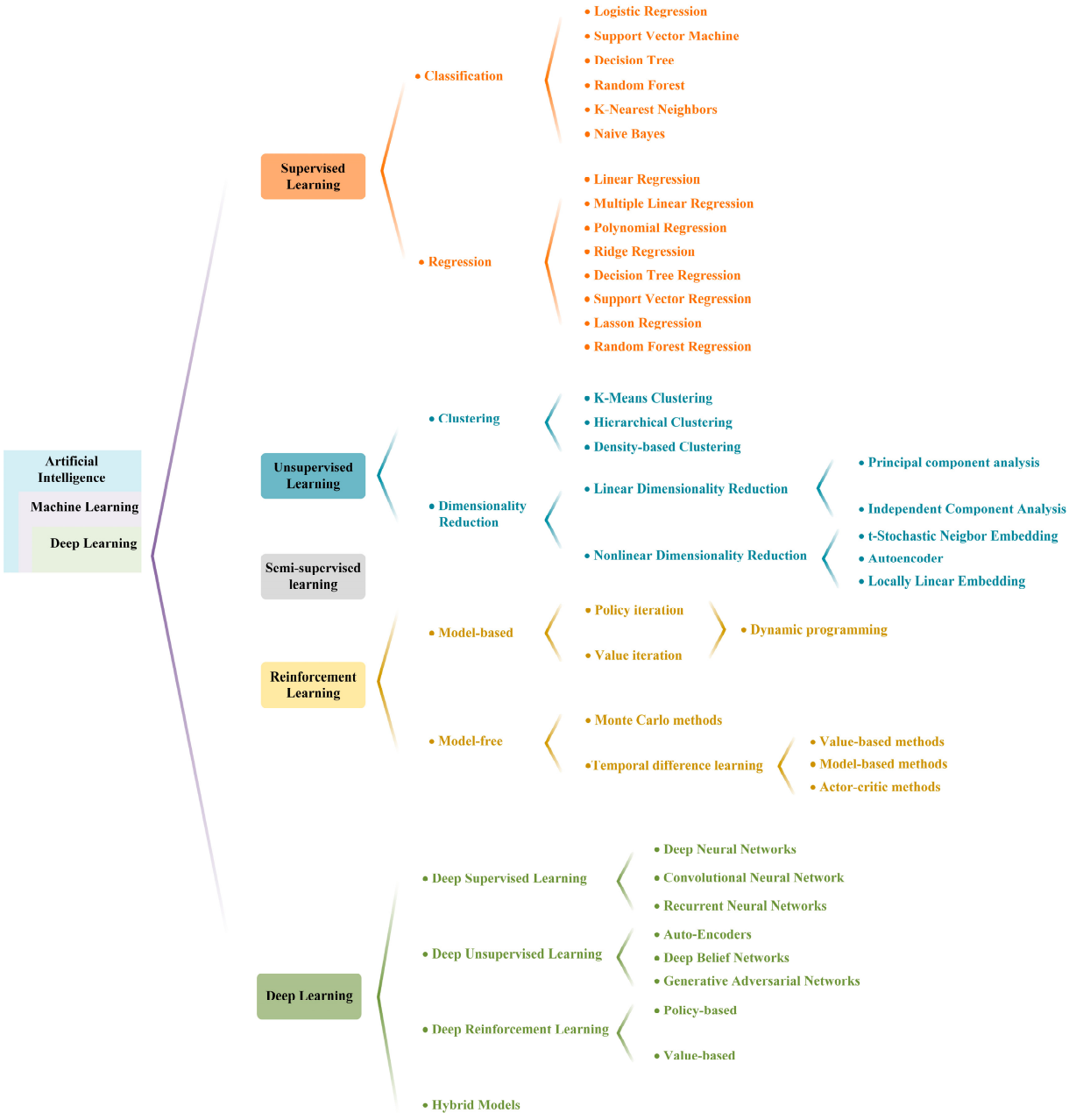

Figure 7. Classification of machine learning algorithms potentially applicable to energy system forecasting [77,121–123].

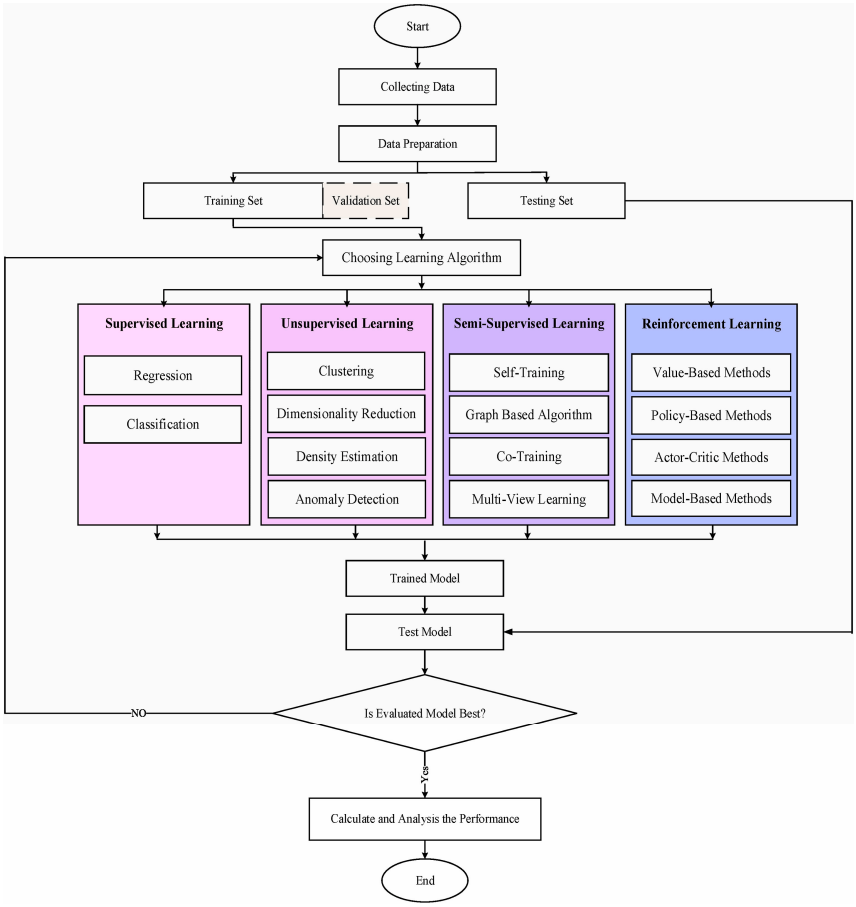

Figure 8. Basic process of machine learning methods [124].

4.3.1. Supervised Learning

Supervised learning models are trained using labeled datasets, where each input sample corresponds to a specific output, enabling the model to learn the general rules for mapping inputs to outputs [125]. Supervised learning can be categorized into classification and regression, depending on the type of the output variables. Classification aims to assign data to predefined classes or categories, with the output typically being a discrete value [124]. Logistic regression is a binary classification method in supervised learning that relies on the Sigmoid function to project the weighted linear combination of features onto a continuous range between 0 and 1 [126]. The logistic regression model is relatively simple with fast training speed, making it well-suited for binary classification tasks. However, it struggles to handle nonlinear problems and its accuracy is generally lower compared to more complex models. Support Vector Machine (SVM) is also a binary classification model that aims to find a hyperplane to separate samples based on the principle of margin maximization [127]. SVMs are suitable for handling complex problems with high-dimensional feature spaces and exhibit relatively higher generalization capabilities. However, they struggle to efficiently handle large-scale training datasets and face challenges in addressing multi-class classification problems. The decision tree [128] represents decision rules and classification outcomes using a tree-like structure, gradually constructing the model by selecting the data features (attributes) that best distinguish different classifications at each partition (node) [126]. The decision tree model has a relatively clear structure and is robust to missing values; however, its generalization ability is relatively limited. Random forest performs classifications by constructing multiple uncorrelated decision trees, primarily based on the Bagging concept, employing the random bootstrap sampling method and an evenly weighted sampling approach [129]. Compared to decision trees, random forests

significantly reduce the risk of overfitting and offer stronger generalization capabilities, demonstrating greater stability and higher accuracy, particularly when dealing with high-dimensional data or complex patterns. Naive Bayes [130] is a representative probabilistic classification algorithm, which fundamentally relies on the Bayes theorem to compute the posterior probability that a sample belongs to each category under specific feature conditions, and assigns the category with the highest posterior probability as the classification result. The basic theory of Bayes is as follows [131]:

$$P(Y = y \mid X = x) = \frac{P(Y = y, X = x)}{P(X = x)} = \frac{P(Y = y)\prod_{i=1}^{n} P(X = x_i \mid Y = y)}{\sum_{i}^{C} P(y_i, X = x)} \quad (1)$$

The core task of K-nearest neighbors (KNN) is to identify the K training samples closest in distance and determine the optimal number of categories. If the K nearest neighbors of a point in the training set all belong to the same category, it can be inferred that the point shares similar characteristics and attributes [132]. The Mahalanobis distance can be calculated to identify the optimal K nearest neighbors.

$$d = D(X, Y) = \sqrt{(x_i - x_j)^T S^{-1} (x_i - x_j)} \quad (2)$$

where X and Y represent two observations from the training set and test set, respectively; x_i and x_j denote two input variables from the same set; and S is the covariance matrix. In addition, the Euclidean Distance, Manhattan Distance, Minkowski Distance, and Chebyshev Distance can also be used as distance metric. However, the optimal value of K needs to be determined through experimentation, which presents certain challenges and complexities.

When the output is a continuous variable rather than a discrete value, it is necessary to employ a regression model [124]. The regression model predicts continuous numerical outputs (output variables) based on input features (input variables) by establishing the following functional relationship [133]:

$$y = f(x_1 \ldots x_n) + e \quad (3)$$

where y represents the actual output, $f(x_1 \ldots x_n)$ denotes the predicted value from the regression model, x_n represents the influencing factors, and e refers to the error term.

Based on the basic framework of the regression model mentioned above, various regression methods and corresponding loss functions L (such as the mean squared error-based loss function) are derived from different mapping functions, as shown in Table 3.

Table 3. Regression models based on different mapping functions.

Methods	Functions	Characteristics	Refs.
Multiple Linear Regression	$y = f(\boldsymbol{x_i}) = \omega_0 + \omega_1 x_1 + \ldots + \omega_n x_n + \varepsilon$ $L(\boldsymbol{\omega}) = \frac{1}{n}\sum_{i=1}^{n}\left(y_i - \left(\boldsymbol{\omega^T x_i} + \omega_0\right)\right)^2$	Assuming that a linear relationship exists between the outcome and the attributes	[134,135]
Polynomial Regression	$y = f(\boldsymbol{x_i}) = \omega_0 + \omega_1 x + \omega_2 x^2 + \ldots + \omega_n x^n + \varepsilon$ $L(\boldsymbol{\omega}) = \frac{1}{n}\sum_{i=1}^{n}\left(y_i - \left(\boldsymbol{\omega^T x_i} + \omega_0\right)\right)^2$	An extension of linear regression in the feature space	[135]
Lasson Regression	$L(\boldsymbol{\omega}) = \frac{1}{n}\sum_{i=1}^{n}\left(y_i - \left(\boldsymbol{\omega^T x_i} + \omega_0\right)\right)^2 + \lambda\|\boldsymbol{\omega}\|_1$	Adding an L1 regularization term to the loss function of linear regression	[136]

Table 3. *Cont.*

Methods	Functions	Characteristics	Refs.
Ridge Regression	$L(\boldsymbol{\omega}) = \frac{1}{n}\sum_{i=1}^{n}\left(y_i - \left(\boldsymbol{\omega}^T\boldsymbol{x_i} + \omega_0\right)\right)^2 + \lambda\|\boldsymbol{\omega}\|_2^2$	Adding an L2 regularization term to loss function of linear regression	[137]
Support Vector Regression	$f(X) = \langle \boldsymbol{\omega}, \boldsymbol{x} \rangle + b$ $L(\boldsymbol{\omega}) = \frac{1}{2}\|\boldsymbol{\omega}\|^2 + C\sum_{i=1}^{n} L(y_i, f(x_i))$	Fitting data by minimizing the loss function $L(\alpha)$	[134,138]
Decision Tree Regression	$y = f(\boldsymbol{x_i}) = \sum_{i=1}^{M} C_i I,\ I = \begin{cases} 1, (x \in R_m) \\ 0, (x \notin R_m) \end{cases}$ $L = \frac{1}{n}\sum_{i=1}^{n}(y_i - f(x_i))^2$	$f(X)$ refers to the predicted output; C_i refers to a constant value associated with the leaf node i; minimizing the mean squared error within a node	[134,139]
Random Forest Regression	-	An ensemble method fitting a definite number of decision trees on parts of the data, and uses their average to improve	[140]

4.3.2. Unsupervised Learning

Compared to supervised learning, unsupervised learning lacks explicit labels for the input data, which needs to independently identify and learn hidden patterns through the structure and relationships within the data, without the aid of labels [141]. Unsupervised learning can be divided into clustering and dimensionality reduction techniques according to the differences in learning tasks.

Clustering involves grouping data samples based on their similarity (typically assessed using distance or similarity metrics) and then leveraging these group patterns to forecast future data. It is assumed that load patterns similar to those that have occurred in the past are likely to recur in the future. Clustering-based methods have been proven to perform well in managing nonlinear and complex patterns, effectively improving the accuracy and robustness of predictions [142].

K-means clustering aims to minimize the squared error between each data point in the dataset and the cluster centroid, subsequently assigning each data point to the nearest cluster center [143]. The objective function J is defined as follows [144]:

$$\text{Min } J = \sum_{j=1}^{k}\sum_{i=1}^{n}\left\|x_i^{(j)} - c_j\right\|^2 \tag{4}$$

where $\left\|x_i^{(j)} - c_j\right\|^2$ represents the distance metric between the selected data point $x_i^{(j)}$; c_j represents the cluster center.

Hierarchical Clustering [145] establishes hierarchical relationships among data based on the dissimilarity or similarity measures between clusters, which can be classified into divisive and agglomerative types. In divisive clustering, all data points are initially treated as a single cluster, which is then iteratively divided into smaller sub-clusters until each cluster contains only one data point or the similarity within the cluster meets a predefined criterion. The agglomerative clustering involves merging individual data points into progressively larger clusters through iterations until all data points are grouped into one cluster or specific criteria is satisfied [144,146]. Density-based clustering [147] is based on the spatial density of the data. When the neighborhood of a point includes a sufficient number of points, the neighboring points are assigned to the same cluster.

Dimensionality reduction techniques aim to map high-dimensional data to a lower-dimensional space while preserving the primary features of the data and reducing redundant information. Principal Component Analysis (PCA) is a widely adopted statistical

dimensionality reduction technique that reduces the dimensionality of data by converting linear combinations of the original variables into a set of new, mutually independent variables, aiming to retain as much overall variance as possible [148]. Independent Component Analysis (ICA) leverages the higher-order statistical properties of data to decompose signals into multiple mutually independent or as-independent-as-possible components [149]. The t-SNE algorithm achieves dimensionality reduction by preserving the similarity of the probability distribution of data points in both low-dimensional and high-dimensional spaces as much as possible. It substitutes the initial Gaussian distribution with a t-distribution in the low-dimensional space, without influencing the high-dimensional space, effectively resolving the crowding issue in the SNE algorithm [150].

4.3.3. Reinforcement Learning

Reinforcement learning involves the interaction between the agent and the environment, where the agent takes actions to receive rewards, continuously adjusting its policy based on a reward and punishment mechanism. The three primary algorithmic approaches for determining the optimal policy in reinforcement learning are dynamic programming, Monte Carlo, and temporal difference methods [121,151].

The most widely used methods in dynamic programming are value iteration and policy iteration. In value iteration, the optimal policy is determined by identifying the optimal value function. On the other hand, policy iteration seeks the optimal policy by iteratively evaluating and improving different policies and retains the policy with the highest cumulative reward. Unlike dynamic programming, the Monte Carlo method does not require a explicit model but estimates the average return of different policies by sampling numerous state–action–reward sequences to find the optimal policy. The Monte Carlo (MC) method allows the agent to learn directly through trial and error without relying on the system model; however, the agent can only update its knowledge base after a complete episode [121]. The temporal difference method combines the characteristics of both Monte Carlo and dynamic programming, which requires no system model and does not need to wait for the completion of an entire sequence to update value estimates. Instead, it updates the estimates at each time step based on the current estimates [152].

4.3.4. Deep Learning

Deep learning evolved from the prediction methods based on artificial neural networks, utilizing the cascading of multiple layers of nonlinear processing units for feature extraction and transformation. The backpropagation algorithm can be used to indicate how a machine should change its internal parameters that are used to compute the representation in each layer from that in the previous layer [153]. Through higher-level abstraction, better scalability, and automatic hierarchical feature learning, deep learning can effectively improve the accuracy of predictions [154,155].

Neural networks are artificial models inspired by biological neurons, simulating a set of interconnected neurons with varying organizational structures, complexities, and types (numbers of neurons, feedback mechanisms, and transformation or activation functions). In each instance, the neural network uses the current weight settings to predict the output based on the input data and evaluates its performance using an error function. If the performance is insufficient, the backpropagation algorithm and Delta rule are employed to adjust the weights to gradually optimize the weight values and bring the predicted values closer to the true values [156]. Additionally, due to the fixed number of input units in a neural network, a recurrent or recursive approach must be adopted to handle the inputs of variable length. Convolutional neural networks are designed to handle data presented as multiple arrays [157], dividing inputs of different lengths into equally sized segments. The

basic structure consists of convolutional layers, pooling layers, and fully connected layers. The convolutional layer focuses on feature extraction, while the pooling layer reduces feature dimensionality, thus lowering the computational complexity [158]. After multiple convolutional and pooling layers, a fully connected layer is typically added, connecting all neurons from the previous layer to those in the current layer to integrate global semantic information. Recurrent neural networks (RNNs) are particularly advantageous for tasks involving sequences [159], as they handle sequential data by using hidden states that can remember previous information and capture long-term dependencies in the sequence. An RNN mainly consists of an input layer, a hidden layer, and an output layer [160]. The input layer primarily receives the input at each time step of the sequence, typically in the form of vectors representing features. The hidden layer is the core component of an RNN, calculating the hidden state at the current time step using the current input and the hidden state from the previous time step and passing it to the next time step. To address the gradient-vanishing issue when processing long time series data in traditional RNNs, a special type of RNN, Long Short-Term Memory (LSTM), was developed. LSTM introduces a unique gating mechanism that controls the information flow through the input gate, output gate, and forget gate. Solar power generation exhibits significant temporal dependencies in terms of sunlight patterns and seasonal variations, and LSTM can effectively capture these temporal relationships, making it well-suited for short-term power prediction. The core of the transformer lies in the self-attention mechanism. With a highly flexible model structure, the transformer is suitable for inputs such as the radiation intensity, temperature, and azimuth, effectively capturing long-term dependencies in the time series data, while offering powerful parallel processing capabilities. Furthermore, to leverage the advantages of different models and enhance the prediction accuracy and stability, multiple methods and models are combined. For example, the LSTM-Transformer model can fully utilize the strengths of both to achieve better performance and more precise predictions.

RNNs and CNNs each have their own limitations when applied to time series forecasting. Standard RNNs usually suffer from the issues of vanishing or exploding gradients when modeling long-term dependencies in sequences, which impairs their ability to effectively capture the influence of earlier time steps on future predictions. Additionally, RNNs cannot be parallelized, resulting in slower training speeds. Furthermore, RNNs have limited responsiveness to real-time scenarios and exhibit poor adaptability to non-stationary changes. CNNs have limitations in modeling time series data and may suffer from the loss of extracted global features.

4.4. Model Assessment

The quantitative evaluation of a model aims to measure its performance in specific tasks, assessing the effectiveness of the trained algorithm and its practical application outcomes. A set of evaluation metrics is usually introduced to quantify the model's performance based on both the training and test sets, preventing insufficient generalization and overfitting issues. The evaluation metrics applicable to various tasks are summarized in Table 4. The performance metrics of some algorithms are shown in Table A3.

Table 4. Quantitative evaluation metrics for machine learning models.

Task Types	Performance Metrics	Explanation	Refs.
Classification	Accuracy rate	$\text{Accuracy} = \frac{true\ positive + true\ negative}{n}$ indicates the proportion of the total number of correct predictions.	[161]
Classification	Precision rate	$\text{Precision} = \frac{true\ positive}{true\ positive + false\ positive}$ indicates the proportion of positive cases that are correctly identified.	[161]
Classification	Recall rate	$\text{Recall} = \frac{true\ positive}{true\ positive + false\ negative}$ indicates the proportion of actual positive cases which are correctly identified.	[161]
Classification	F_1 score	$F_1 = \frac{2 \times Precision \times Recall}{Precision + Recall}$ F_1 is a comprehensive metric that balances precision and recall in the cases of class imbalance.	[161]
Classification	Specificity	$\text{Specificity} = \frac{true\ negative}{false\ positive + true\ negative}$ Indicates the proportion of actual negative cases that are correctly identified.	[161]
Classification	Matthews' correlation coefficient (MCC)	$\text{MCC} = \frac{TN \cdot TP - FN \cdot FP}{\sqrt{(TP+FP)(TP+FN)(TN+FP)(TN+FN)}}$ MCC measures the correlation between the real and the predicted values of the instances.	[162]
Regression	Mean Bias Error (MBE)	$MBE = \frac{1}{N}\sum_{i=1}^{N}\left\lvert P_{\text{pred}} - P_{\text{meas}}\right\rvert$ MBE measures the average bias between predicted and actual values.	[163]
Regression	Standard Deviation of Errors (SDE)	$SDE = \sqrt{\frac{1}{N}\sum_{i=1}^{N}\left(P_{\text{pred}} - P_{\text{meas}} - MBE\right)^2}$ SDE measures the variability of the prediction errors around the mean error.	[163]
Regression	Mean Absolute Error (MAE)	$MAE = \frac{1}{N}\sum_{i=1}^{N}\lvert t_i - T_i\rvert$, MAE measures the average of the absolute difference between the prediction errors.	[164,165]
Regression	Mean Square Error (MSE)	$MSE = \frac{1}{N}\sum_{i=1}^{N}(t_i - T_i)^2$, MSE measures the average squares of the prediction errors.	[164,165]
Regression	Root Mean Square Error (RMSE)	$RMSE = \sqrt{MSE} = \sqrt{\frac{1}{N}\sum_{i=1}^{N}(t_i - T_i)^2}$ $RMSE$ measures the standard deviation of the prediction errors.	[163,164]
Regression	Mean Absolute Percentage Error (MAPE)	$MAPE = \frac{1}{N}\sum_{i=1}^{N}\left\lvert\frac{t_i - T_i}{T_i}\right\rvert$, $MAPE$ measures the average percentage error between predicted and actual values.	[163,164]
Regression	Relative Squared Error	$RSE = \frac{\sum_{i=1}^{n}\left(Y_i - \hat{Y}_i\right)^2}{\sum_{i=1}^{n}\left(Y_i - \overline{Y}_i\right)^2}$ RSE measures the lack of fit.	[161]
Regression	R^2	$R^2 = 1 - \frac{\sum_{i=1}^{N}(t_i - T_i)^2}{\sum_{i=1}^{N}\left(t_i - \overline{T}\right)^2}$ R^2 reflects the explanatory power of the model.	[161,165]
Regression	Normalized RMSE (NRMSE)	$NRMSE = \frac{\sqrt{\frac{1}{N}\sum_{i=1}^{N}(t_i - T_i)^2}}{T_{max} - T_{min}}$ $NRMSE$ represents the normalized form of $RMSE$.	[161]

Table 4. *Cont.*

Task Types	Performance Metrics	Explanation	Refs.
Clustering	Davies–Bouldin index	$DB = \frac{1}{c}\sum_{i=1}^{c} max_{i\neq j}\left\{\frac{d(X_i)+d\left(X_j\right)}{d\left(c_i,c_j\right)}\right\}$ DB measures clustering quality by evaluating the ratio between the sum of within-cluster scatter and between-cluster separation.	[164]
Clustering	Dunn index	$Dunn = min_{1\leq i\leq c}\left\{min\frac{d\left(c_i,c_j\right)}{max_{1\leq k\leq c}d(X_k)}\right\}$ The $Dunn$ index measures the clustering quality based on the inter-cluster distance and the intra-cluster distance.	[164]
Clustering	Rand index	$R = \frac{\lvert SS\rvert+\lvert DD\rvert}{\lvert SS\rvert+\lvert SD\rvert+\lvert DS\rvert+\lvert DD\rvert}$ R reflects the proportion of correct decisions, assigning equal penalties to both false negative and false positive errors.	[166]
Clustering	Fowlkes and Mallows index (FM)	$FM = \sqrt{\frac{\lvert SS\rvert}{\lvert SS\rvert+\lvert SD\rvert}\times\frac{\lvert SS\rvert}{\lvert SS\rvert+\lvert DS\rvert}}$ A higher FM value indicates stronger alignment between the clustering and the reference standard.	[166]
Clustering	Jaccard coefficient	$J = \frac{\lvert SS\rvert}{\lvert SS\rvert+\lvert SD\rvert+\lvert DS\rvert}$ J measures the similarity of clustering.	[166]
Others	Forecast skill score (FS)	$U = \sqrt{\frac{1}{N}\sum_{i=1}^{N}\left(\frac{P_{\mathrm{pred},t}-P_{\mathrm{meas},t}}{P_{\mathrm{cs},t}}\right)^2}$ $V = \sqrt{\frac{1}{N}\sum_{i=1}^{N}(\Delta k(t))^2}$ $FS = 1-\frac{U}{V}$ FS measures the improvement in model performance compared to the reference model.	[163]

5. Modeling Technologies for Intelligent Optimization and Scheduling

Various modeling techniques have been developed, such as the steady-state and dynamic modeling of power systems, as well as the grid characteristic and control model, to characterize the operational characteristics, response mechanisms, and scheduling strategies of microgrids under different operating conditions. This section primarily focuses on the analysis of microgrid scheduling technologies and their applications [167]. In order to present a universal modeling framework for microgrid scheduling, typical models and methodologies from different studies are integrated and generalized into a representative modeling architecture, as illustrated in Figure 9. First, the fundamental components of the microgrid are identified based on the specific scenario, and the primary functional requirements of the microgrid model are clarified. Accordingly, relevant datasets are selected and formulated, including the raw data, data preprocessing process, and necessary data forecasting. Subsequently, the basic structure of the scheduling model should be established, which involves defining the operational rules, strategies, and modeling approaches. In addition, the actual model construction phase is carried out, where mathematical models for the core components are developed, appropriate optimization objectives are selected, and comprehensive constraints are defined in alignment with practical needs and existing studies.

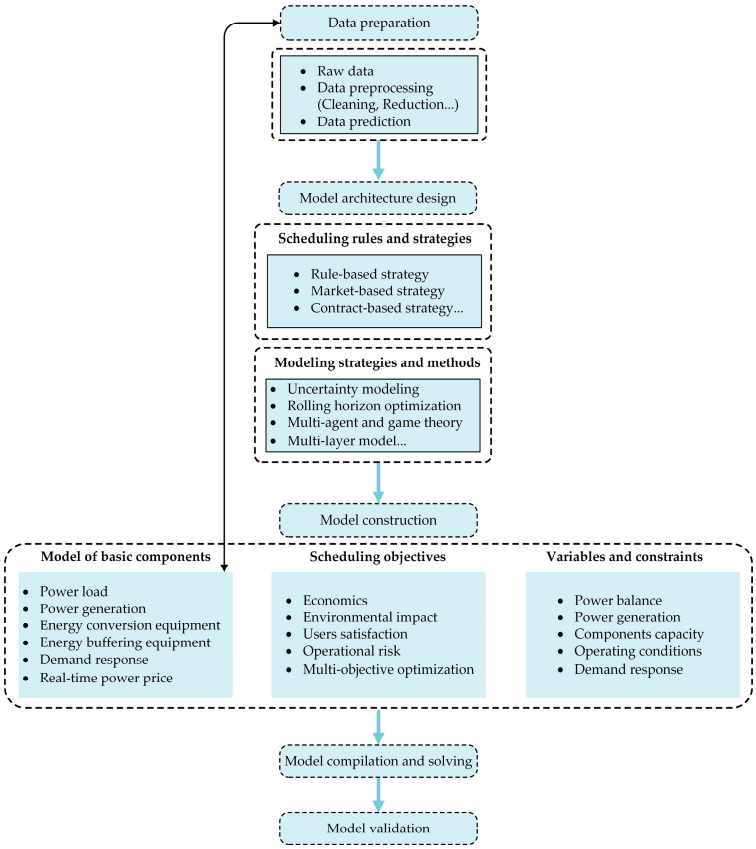

Figure 9. Basic process of microgrid scheduling model.

5.1. Model of Basic Components in Microgrids

Different microgrid systems involve multiple physical and virtual components. This section summarizes the potential components and their corresponding models. During the modeling process, it is necessary to select and match them based on actual conditions, with these sub-models integrated into the microgrid scheduling model.

(1) Modeling of load

The electrical load is determined by the power consumption of various power-consuming devices in industrial systems. These devices may either start and stop frequently or operate continuously due to process constraints, potentially resulting in demand peaks of varying intensity at different time periods [168]. Various modeling methods can be applied based on the load characteristics, including constant loads, time-varying loads, and both schedulable and non-schedulable loads [169–174]. Some studies employ a time series to characterize load variations and simulate load fluctuations using normal distribution properties [175–177]:

$$f_l\left(P^L\right) = \frac{1}{\sqrt{2\pi}\sigma_L}\exp\left(-\frac{\left(P^L-\mu_L\right)^2}{2{\sigma_L}^2}\right) \quad (5)$$

where P^L represents the load power; μ_L and σ_L are the mean and standard deviation of load power.

(2) Modeling of power-generation equipment

The power output of the solar photovoltaic system can be expressed as follows [167,168,176,178–180]:

$$P_{\mathrm{PV}}^{(t)} = P_{\mathrm{PV}}^{\mathrm{Rated}} \frac{G_{\mathrm{PV}}^{(t)}}{G_{\mathrm{AT}}^{(t)}} \left[1 + K\left(T_{\mathrm{PV}}^{(t)} - T_{\mathrm{PV}}^{\mathrm{RT}}\right)\right] \tag{6}$$

where $P_{\mathrm{PV}}^{(t)}$ represents the power output at time t, $P_{\mathrm{PV}}^{\mathrm{Rated}}$ is the rated power output, $G_{\mathrm{AT}}^{(t)}$ represents the reference irradiance, $T_{\mathrm{PV}}^{\mathrm{RT}}$ represents the reference temperature, and K is the power-temperature coefficient, 0.0047 $^{\circ}\mathrm{C}^{-1}$.

The temperature of the photovoltaic panel can be expressed as follows:

$$T_{\mathrm{PV}}^{(t)} = T_{\mathrm{AT}}^{(t)} + 0.0138\left(1 + 0.031T_{\mathrm{AT}}^{(t)}\right)\left(1 - 0.042V_{\mathrm{PV}}^{(t)}\right)G_{\mathrm{PV}}^{(t)} \tag{7}$$

where $T_{\mathrm{PV}}^{(t)}$ refers to the temperature of the photovoltaic panel at time t, $T_{\mathrm{AT}}^{(t)}$ is the ambient temperature at time t, $V_{\mathrm{PV}}^{(t)}$ represents the wind speed at time t, and $G_{\mathrm{PV}}^{(t)}$ is the solar irradiance at time t, W/m^2.

The output current of the photovoltaic cell can be expressed as follows:

$$I = I_{ph} - I_0\left[\exp\left(\frac{q(V + IR_S)}{nkT}\right) - 1\right] - \frac{V + IR_S}{R_P} \tag{8}$$

where I_{ph} represents the photocurrent caused by irradiance, I_0 is the diode saturation current, V represents the voltage of cell, q represents the charge, n is the diode ideality factor, k is the Boltzmann constant, T is the cell temperature, R_S is the series resistance, and R_P is the shunt resistance.

The power output of the wind turbine can be expressed by the following [176,179,181]:

$$P_{\mathrm{WT}}^{(t)} = \begin{cases} 0, v_{\mathrm{W}}^{(t)} < v_{\mathrm{cut-in}} \\ P_{\mathrm{WT}}^{\mathrm{R}} \frac{v_{\mathrm{W}}^{(t)} - v_{\mathrm{cut-in}}}{v_{\mathrm{rws}} - v_{\mathrm{cut-in}}}, v_{\mathrm{cut-in}} \le v_t < v_{\mathrm{rws}} \\ P_{\mathrm{WT}}^{\mathrm{R}}, v_{\mathrm{rws}} \le v_t < v_{\mathrm{cut-out}} \\ 0,\ v_{\mathrm{W}}^{(t)} > v_{\mathrm{cut-out}} \end{cases} \tag{9}$$

$$v_{\mathrm{W}}^{(t)} = v_{\mathrm{R}}^{(t)}\left(\frac{H_{\mathrm{WT}}}{H_{\mathrm{R}}}\right)^{\gamma} \tag{10}$$

where $v_{\mathrm{W}}^{(t)}$ is the wind speed at the hub height at time t; $v_{\mathrm{R}}^{(t)}$ is the wind speed at the height of anemometer tower; H_{WT} is the height of hub; H_{R} is the height of anemometer tower; γ is the friction coefficient, γ = 1/7; $P_{\mathrm{WT}}^{\mathrm{R}}$ is the rated power of the wind turbine; $v_{\mathrm{W}}^{(t)}$ is the actual wind speed at time t; $v_{\mathrm{cut-in}}$ is the cut-in speed; v_{rws} is the rated wind speed; and $v_{\mathrm{cut-out}}$ is the cut-out speed.

(3) Modeling of energy conversion equipment

The micro turbine can be calculated by the following [182,183]:

$$P_{\mathrm{GT}}(t) = \eta_{\mathrm{GT-P}} \cdot LHV \cdot G_{\mathrm{GT}}(t) \tag{11}$$

$$H_{\mathrm{GT}}(t) = G_{\mathrm{GT}}(t) \cdot LHV \cdot (1 - \eta_{\mathrm{GT-P}} - \eta_{\mathrm{GT-loss}}) \tag{12}$$

where $P_{GT}(t)$ is the power generated by the gas turbine at time t, kW; $G_{GT}(t)$ is the amount of natural gas consumed by the gas turbine at time t, m^3; LHV is the lower heating value of the gas, kW·h/m^3; $H_{GT}(t)$ is the thermal energy produced by the gas turbine at time t, kW;

and η_{GT-P} and $\eta_{GT-loss}$ represent the power generation efficiency and gas loss rate of the gas turbine, respectively.

The thermal output of a waste heat boiler can be expressed as follows [178]:

$$q_{h,t}^{\mathrm{whb}} = \eta_h^{whb}\left(1-\eta_e^{gt}\right)q_t^{gt}\varphi_{\mathrm{g}} \tag{13}$$

where $q_{h,t}^{whb}$ represents the thermal power output of the waste heat boiler at time t; η_h^{whb} represents the efficiency of the waste heat boiler.

The Combined Heat and Power (CHP) system utilizes a gas turbine integrated with waste heat boilers to simultaneously generate electrical and thermal energy, achieving an overall efficiency of 70% to 90%. The electrical power output and thermal output at time t are expressed as follows [184]:

$$\varphi_{\mathrm{CGT}} = a\left(\frac{P_{\mathrm{CGT},t}}{P_{\mathrm{CGT}}^{\max}}\right)^3 - b\left(\frac{P_{\mathrm{CGT},t}}{P_{\mathrm{CGT}}^{\max}}\right)^2 + c\frac{P_{\mathrm{CGT},t}}{P_{\mathrm{CGT}}^{\max}} + d \tag{14}$$

$$P_{\mathrm{CGT},t} = \varphi_{\mathrm{CGT}}Q_{\mathrm{CGT},t}^{g}G_{\mathrm{g}} \tag{15}$$

$$H_{\mathrm{CGT},t} = \frac{1-\varphi_{\mathrm{CGT}}-\mu_{\mathrm{CGT}}^{\mathrm{loss}}}{\varphi_{\mathrm{CGT}}}P_{\mathrm{CGT},t} \tag{16}$$

$$H_{\mathrm{WHB},t} = \sum_{i=\frac{\mathrm{CGT}}{\mathrm{TP}}} H_{i,t}\mu_{\mathrm{WHB}}COP_{\mathrm{WHB}} \tag{17}$$

where the a, b, c, and d represent quadratic regression coefficients for turbine efficiency curves; $P_{\mathrm{CGT},t}$ represents rated capacity of gas turbines; φ_{CGT} and $\mu_{\mathrm{CGT}}^{\mathrm{loss}}$ represent the energy efficiency and loss rate of gas turbines, respectively; $Q_{\mathrm{CGT},t}^{g}$ represents fuel consumption; G_{g} represents the lower heating value of the consumed fuel; $H_{\mathrm{CGT},t}$ refers to the thermal output; $H_{i,t}$ represent the waste heat from the upstream device i at time t, respectively; μ_{WHB} represents the efficiency of thermal exchange; and COP_{WHB} represents the efficiency of thermal recovery.

The electric heat pump can convert electricity power to thermal energy directly, which can be expressed by the following [185]:

$$H_{t,i}^{\mathrm{EHP}} = \sigma_{\mathrm{EHP}}^{\mathrm{p2h}}P_{t,i}^{\mathrm{EHP}} \tag{18}$$

where $H_{t,i}^{\mathrm{EHP}}$ represents the thermal output of the EHP system, $P_{t,i}^{\mathrm{EHP}}$ represents the consumed power, and $\sigma_{\mathrm{EHP}}^{\mathrm{p2h}}$ is the conversion coefficient.

(4) Modeling of energy buffering equipment

Energy storage devices can effectively balance the power supply and demand in industrial microgrid systems and enhance their stability. The capacity of the energy storage battery can be calculated by the following [168]:

$$B_{\mathrm{capacity}} = \frac{E_{\mathrm{load}} \times Days_{\mathrm{off}}}{DoD_{\max} \times \eta_{\mathrm{temp}}} \tag{19}$$

where E_{load} is the load that needs to be supplied during unavailability of power, $Days_{\mathrm{off}}$ is the storage days (power from the electric grid is unavailable), $DoD_{\max}$ is the maximum depth of discharge of the battery, and η_{temp} is the temperature corrector factor.

The state of energy storage device can be described as follows [186]:

$$E_{\mathrm{ES}}(t+1) = E_{\mathrm{ES}}(t) + P_{\mathrm{ES,ch}}(t)\Delta t\eta_{\mathrm{ES,ch}} + \frac{P_{\mathrm{ES,dis}}(t)\Delta t}{\eta_{\mathrm{ES,dis}}} \tag{20}$$

where $E_{ES}(t+1)$ and $E_{ES}(t)$ represent the energy storage states at time $t+1$ and time t, respectively; $P_{ES,ch}(t)$ and $\eta_{ES,ch}$ refer to the charging power and efficiency of the energy storage device, respectively; and $P_{ES,dis}(t)$ and $\eta_{ES,dis}$ refer to the discharge power and efficiency of the energy storage device, respectively.

SOC describes the state of the charge, which can be calculated by the following:

$$SOC_{BT}(t) = \frac{E_{ES}(t)}{B_{capacity}} \tag{21}$$

where $E_{ES}(t)$ represents the energy stored in the energy storage device at time t; $B_{capacity}$ is the total storage capacity of the battery.

Alkaline electrolyzers are capable of handling significant power fluctuations, operating stably within 10% to 100% of the rated power, and can also be used for absorbing excess power. The operating voltage of the alkaline electrolyzer can be described as follows [187,188]:

$$U_{cell} = U_{rev} + \frac{R_1 + R_2 T_k}{A} I_{el} + \left(s_1 + s_2 + s_3 {T_k}^2\right) \log\left(\frac{t_1 + \frac{t_2}{T_k} + \frac{t_3}{{T_k}^2}}{A} I_{el} + 1\right) \tag{22}$$

$$U_{rev} = \frac{\Delta G}{zF} \tag{23}$$

$$U_{rev} = N \times U_{cell} \tag{24}$$

The electrolysis efficiency of the electrolyzer can be expressed as follows:

$$\eta_e = \frac{U_{th}}{U_{el}} \tag{25}$$

$$\eta_f = 96.5 e^{\left(\frac{0.09}{I_{el}} - \frac{75.5}{{I_{el}}^2}\right)} \tag{26}$$

$$\eta = \eta_e \times \eta_f \tag{27}$$

where η represents the electrolysis efficiency, η_f is the Faraday efficiency, and η_e is the voltage efficiency.

The pressure of the hydrogen produced via electrolysis is not suitable for storage and requires compression to an appropriate pressure by a compressor. The compressor model can be described as follows [187]:

$$P_Y = \frac{RLT_{in}\theta}{\eta_Y(\theta - 1)} \left[\left(\frac{P_{out}}{P_{in}}\right)^{\frac{\theta-1}{\theta}} - 1\right] \tag{28}$$

where R represents the specific heat capacity of hydrogen, L refers to the flow rate of hydrogen in the compressor, T_{in} is the temperature of hydrogen entering the compressor, η_Y is the efficiency of the compressor, θ represents the isentropic index of hydrogen, and P_{in} and P_{out} are, respectively, the input and output pressure of hydrogen.

Fuel cells [189] can convert hydrogen into electrical or chemical energy. The proton exchange fuel cells are characterized by low costs and fast response times, and their output power can be calculated according to Equation (29) [181]. The more detailed fuel cell modeling methods can be referenced in [190,191].

$$P_{FC}^t = V_{FC}^t H_{HHV} \eta_{FC} \tag{29}$$

where P_{FC}^{t} is the output power of the fuel cell at time t, MW; V_{FC}^{t} is the amount of hydrogen input of the fuel cell at time t, kg; H_{HHV} represents the higher heating value of hydrogen; and η_{FC} is the conversion efficiency of the fuel cell.

The hydrogen storage system stores the hydrogen generated during electrolysis in the hydrogen storage tank and supplies it to the fuel cell for power generation when necessary. The energy balance model of the hydrogen storage can be expressed by the following [181]:

$$S_{H_2}^{t} = S_{H_2}^{t-1}\eta_S + V_{H_2}^{t}\eta_{cha} - \frac{V_{FC}^{t} + V_{Fsell}^{t}}{\eta_{dis}} \tag{30}$$

where $S_{H_2}^{t}$ is the remaining hydrogen volume in the hydrogen storage tank at time t, $V_{H_2}^{t}$ is the amount of hydrogen sold at time t, η_S is storage efficiency of hydrogen storage tank, and η_{cha} and η_{dis} are, respectively, the efficiency of hydrogen input and hydrogen output.

Furthermore, with the increasing popularity of electric vehicles, they have become a crucial part of peak shaving in industrial microgrids, as indicated in [192,193].

(5) Modeling of demand response

The demand response unit can dynamically align multiple energy loads with renewable generation profiles, market signals, and the grid's incentive instructions, which aims to optimize operational costs while maintaining grid stability. The total load shifted by the demand response is as follows [194]:

$$P_{DR}^{t} = \left[Load_{base}^{t} - Load_{DR}^{t}\right] \cdot \Delta t \tag{31}$$

$$Load_{DR}^{t} = \left[DR_t \times Load_{base}^{t}\right] \cdot \Delta t \tag{32}$$

$$0 \le DR_t \le 1 \tag{33}$$

The price-based demand response is typically based on market prices, guiding users to adjust their consumption patterns through load shifting (characterized by cross-elasticity coefficients) and load curtailment (characterized by self-elasticity coefficients). The load variation can be expressed as follows [184,195,196]:

$$\Delta L_{PB,t}^{z} = L_t^z \cdot \left\{ e_{tt}^{z} \cdot \frac{\Delta \xi_t^z}{\xi_t^z} + \sum_{s=1}^{24} e_{st}^{z} \cdot \frac{\Delta \xi_s^z}{\xi_s^z} \right\}, z = power, gas, heat \tag{34}$$

$$e_{st}^{z} = \frac{\frac{\Delta L_s^z}{L_s^z}}{\frac{\Delta \xi_t^z}{\xi_t^z}}, \begin{cases} e_{tt} \le 0, \ if \ s = t \\ e_{tt} \ge 0, \ if \ s \ne t \end{cases} \tag{35}$$

where e_{tt} and e_{st} represent the self-elasticity (intra-temporal) and cross-elasticity (inter-temporal) coefficients, respectively; L_t^z represents the multiple energy load (electricity, gas, and heat) at time t; L_s^z and ΔL_s^z represent the baseline load and the load variation after the price-based demand response, respectively; and $\Delta \xi_t^z$ and $\Delta \xi_t^z$ represent the baseline energy price and the price variation, respectively.

An incentive-based demand response encourages users to participate in the ancillary services market through contractual agreements and emergency load adjustments. The incentive load adjustment can be expressed as follows [184]:

$$\Delta L_{IB,t}^{z} = \Delta L_{IB,t}^{z,c} + \sum_{k=1}^{K} \left(\Delta L_{IB,k,t}^{z,u} + \Delta L_{IB,k,t}^{z,d} \right) \tag{36}$$

where $\Delta L_{\mathrm{IB},t}^{z,c}$ represents the load adjustment committed through the contract, $\Delta L_{\mathrm{IB},k,t}^{z,u}$ and $\Delta L_{\mathrm{IB},k,t}^{z,d}$ represent the incremental/decremental emergency load adjustments at regulation step k, and K represents the number of discrete regulation steps.

(6) Modeling of real-time power price

The reasonable pricing mechanism contributes to maintaining the balance between the electricity supply and demand, facilitates the integration of clean energy, and promotes the efficient allocation of electricity resources. In general, the time-of-use electricity pricing mechanism is commonly applied in industrial scenarios, which is divided into five periods nationwide: peak, high-peak, mid-peak, off-peak, and deep off-peak [197]. In addition, some studies also conducted real-time pricing based on marginal costs. A typical electricity pricing model can be described as follows [198,199]:

$$C_{\mathrm{outpower},i,t} = a_i P_{i,t}^2 + b_i P_{i,t} + c_i \tag{37}$$

$$B_{i,t} = UF_{i,t} - C_{\mathrm{outpower},i,t} - MCP_{i,t}\Delta P_{i,t} \tag{38}$$

$$\frac{dB_{i,t}}{dP_{i,t}} = -\frac{d\left(C_{\mathrm{outpower},i,t}\right)}{dP_{i,t}} + MCP_{i,t} = 0 \tag{39}$$

$$MCP_{i,t} = MC_{i,t} \tag{40}$$

$$SP_t \le MCP_{i,t} \le BP_t \tag{41}$$

where $C_{\mathrm{outpower},i,t}$ is the cost of non-controllable and controllable power generation; a_i, b_i, and c_i are the cost factor; $B_{i,t}$ represents the income from the purchase and sale of electricity; $UF_{i,t}$ represents the utility function; $\Delta P_{i,t}$ represents the generating capacity of the generator at time t; $MC_{i,t}$ is the marginal costs at time t; and SP_t and BP_t are the electricity selling and buying price from microgrid to power distribution network at time t.

5.2. Scheduling Rules and Strategies of Microgrids

The principles and methods for power allocation and scheduling should be defined in advance to ensure the dynamic management of power interactions in a microgrid scheduling model. The rule-based strategy aims to perform scheduling according to predefined rules, making decisions based on a set of monitoring conditions (net demand, state of charge, etc.) and their corresponding predefined response patterns [200]. For example, the scheduling strategy may involve the prioritization of critical and non-critical loads, as well as the prioritization of frequency and voltage stability. The market-based strategy aims to optimize power production and matching through market price signals, such as scheduling based on real-time or day-ahead prices of electricity. The contract-based strategy aims to execute and schedule according to the contracts established between multiple agents [201]. Some typical studies depicting different scheduling modes of microgrids are shown in Table A2.

5.3. Typical Modeling Strategies and Methods

(1) Uncertainty modeling

Renewable energy holds the potential to offer reserve capacity, but its intrinsic uncertainty or prediction error may affect the stability of this service, which should be adequately considered during the scheduling process. A series of targeted modeling approaches, such as probabilistic models, stochastic optimization, robust optimization, fuzzy optimization, IGDT, and Monte Carlo simulation [202–204], have been developed to address uncertainty-related issues. The relatively classical approaches are robust optimization (RO) [205,206] and stochastic optimization (SO) [207,208], with the former assuming that uncertainty fol-

lows a predefined probability distribution, while the latter typically makes decisions based on the worst-case scenario. The technical challenge of stochastic programming lies in the difficulty of precisely describing the uncertain parameters and the probability distributions of scenarios. Furthermore, as the number of scenarios increases, the computational complexity and costs grow significantly. Reducing the number of scenarios may lead to insufficient robustness and inadequate feature representation [209,210]. Robust optimization does not necessitate a prior understanding of the probability distribution of uncertain variables, though traditional robust optimization methods typically lead to relatively conservative results. Therefore, the robust optimization methods have been continuously improved, including distribution robust optimization (DRO), data-driven distribution robust optimization (DDRO), and hybrid robust optimization (HyRO) [211]. Uncertain meteorological conditions, such as sunlight, introduce significant uncertainty in solving the optimization scheduling problem for photovoltaic power generation. In stochastic programming, typical solar radiation scenarios can be extracted and probability distributions can be analyzed based on historical cloud data. For each corresponding scenario, optimization scheduling is performed using the relevant probability distribution. On the other hand, robust optimization determines ranges of key parameters based on historical cloud data and constructs the corresponding robust optimization scheduling model.

(2) Rolling horizon optimization

Rolling optimization is a dynamic time series decision-making approach characterized by three key parameters: the rolling horizon determines the size of the rolling window or optimization horizon, the moving interval indicates the time distance that rolling windows move forward, and the decision step [212–214]. Yang et al. [215] employed a model predictive of a control-based rolling optimization mechanism to address the intraday scheduling of microgrids, which iteratively converges to an optimal solution within a finite time horizon while continuously shifting the optimization window forward to the next stage. To address the coordination challenge between power smoothing and scheduling optimization arising from the disparity between optimization timescales and actual power fluctuations, Li et al. [212] adopted a novel rolling optimization strategy, which dynamically adjusts the optimization horizon and applies real-time corrections to mitigate deviations effectively.

(3) Multi-agent and game theory

As the number of electricity users grows, ensuring cooperation and optimal operation among multiple stakeholders becomes essential. Multi-agent systems are typically composed of multiple interactive agents, and their distributed nature facilitates the application of decentralized strategies in energy management systems [203]. Smart agents exhibit three fundamental properties: responsiveness (environmental awareness and reaction), proactiveness (autonomous decision-making based on goals), and social interaction ability (engaging with other agents through cooperation or competition) [216]. Game theory [217] is frequently introduced into the decision-making process to fully comprehensively consider multi-agent interactions and enhance their operational strategies, achieving global optimization and equilibrium. The game process can be categorized into cooperative and non-cooperative games, dynamic and static games, as well as complete and incomplete information games. Wang et al. [218] developed an optimization method for microgrid clusters using multi-agent deep reinforcement learning (MADRL), representing the scheduling optimization problem as a Markov game with an unknown state transition probability function. Jin et al. [219] constructed a microgrid structure based on a multi-agent system, derived the Nash equilibrium using a particle swarm optimization method, and compared the optimization results of cooperative and non-cooperative games.

(4) Multi-layer model

To reduce model complexity and enhance computational efficiency, some studies decompose the global optimization problem of microgrid scheduling into multiple stages, thereby mitigating excessive computational costs. Tan et al. [220] proposed a two-stage robust scheduling model for multiple microgrid systems with electric vehicle loads, employing the column and constraint generation algorithm to solve the robust dispatch problem through the mutual iteration of two main problems and sub-problems. Jani et al. [221] developed a two-stage multi-time scale model considering both day-ahead and real-time markets, with the day-ahead market formulated as two-layer model to reduce the operating cost of system. Ning et al. [222] developed a two-layer optimal scheduling method for multi-energy virtual power plant with source-load synergy, in which the upper layer mainly focused on optimizing the load side by utilizing the time-of-use price and dispatching controllable loads, while the lower layer optimizes the power output of each distributed power source based on the upper layer model.

5.4. Modeling of Optimal Scheduling for Microgrids

This section provides a relatively comprehensive overview of potential optimization objectives and constraints that may be involved in microgrid scheduling models, allowing for the selection and combination based on specific requirements. For economic objectives, various cost and benefit calculation methods are presented, enabling the total cost and total benefit to be determined by aggregating individual cost and revenue components. In addition, objectives related to the environmental impact, user satisfaction, and system operational risk, along with their possible calculation methods, are also provided. Furthermore, multi-objective optimization approaches can be employed to balance the trade-offs among the above objectives.

5.4.1. Scheduling Objectives

(1) Objective for enhancing operational economics

The economic performance of microgrid systems is currently the dominant scheduling objective, primarily focusing on the costs and revenues associated with the energy supply, storage, distribution, and management within the microgrid. Numerous studies conducted scheduling based on minimizing the operating costs or maximizing the revenues of microgrids. The microgrid's main components of cost and revenue are shown in Table 5.

Table 5. Composition of microgrid operational costs and profits.

Cost	Calculation Methods	Ref.
Costs of energy purchase for power generation	$C_{\text{energy,buy}}(t) = \sum_{t=1}^{T} \mu_{\text{buy}}(t) \cdot G_{\text{buy}}(t) \Delta t$	[223]
Costs of curtailment penalties for renewable energy	$C_{\text{MG}}^{\text{AB},s} = \sum_{t=1}^{T} \left[\xi_{\text{ab}} P_{\text{AB},t}^{s} \right] \Delta t$	[184]
Cost of operational maintenance (distributed power generation)	$ADCC_i = c_{\text{cost},i} \frac{r_i (1+r_i)^{l_i}}{(1+r_i)^{l_i} - 1}$ $C_{\text{om}} = \sum_{T=1}^{T} \sum_{i=1}^{N} K_{\text{om},i} P_i(t) \Delta t$ $C_{\text{dp}} = \sum_{T=1}^{T} \sum_{i=1}^{N} \frac{ADCC_i}{P_{cci} \times 8760 \times k_i} P_i(t) \Delta t$	[192]

Table 5. *Cont.*

Cost	Calculation Methods	Ref.
Cost of maintenance (energy transmission equipment and energy storage equipment)	$C_{\mathrm{om}} = \sum_{T=1}^{T}\left(\mu_{\mathrm{gt}}P_t^{\mathrm{gt}} + \mu_{\mathrm{gb}}H_t^{\mathrm{gb}} + \mu_{\mathrm{p2g}}G_t^{\mathrm{p2g}}\right)\Delta t + \sum_{T=1}^{T}\left[v_{\mathrm{es}}\left(P_t^{\mathrm{ch}} + P_t^{\mathrm{dis}}\right) + v_{\mathrm{hs}}\left(H_t^{\mathrm{ch}} + H_t^{\mathrm{dis}}\right) + v_{\mathrm{gs}}\left(G_t^{\mathrm{ch}} + G_t^{\mathrm{dis}}\right)\right]\Delta t$	[223]
Cost of controllable unit start-stop cost	$C_{\mathrm{SS}}^{t} = \sum_{j=1}^{J}\max\left[0, \sigma_j^t - \sigma_j^{t-1}\right]C_{\mathrm{SS},j}^{\mathrm{U}}$	[224]
Cost of trading (transactional costs with the main grid)	$C_{\mathrm{grid}} = \sum_{t=1}^{T}\left(C_{\mathrm{buy}}(t) - C_{\mathrm{sell}}(t)\right)\Delta t = \sum_{t=1}^{T}\left(c_{\mathrm{buy}}(t)\cdot P_{\mathrm{buy}}(t) - c_{\mathrm{sell}}(t)\cdot P_{\mathrm{sell}}(t)\right)\Delta t$	[192,225]
Cost of comprehensive demand response	$C_{\mathrm{MG}}^{\mathrm{DR},S} = \sum_{z}\sum_{t=1}^{T}\sum_{k=1}^{K}\left[(\xi_t^z + \Delta\xi_t^z)\left(L_t^z + \Delta L_{\mathrm{PB},t}^z\right) - \xi_t^z L_t^z + \xi_t^{z,c}\Delta L_{\mathrm{IB},t}^{z,c} + \left(\xi_{k,t}^{z,u}\Delta L_{\mathrm{IB},k,t}^{z,u} + \xi_{k,t}^{z,d}\Delta L_{\mathrm{IB},k,t}^{z,d}\right)\right]$	[184,226]
Cost of peak–valley difference	$C_{\mathrm{s}}^{\mathrm{PD}} = \left(\max_{t=1,\ldots,T}\left(P_{s,t}^{\mathrm{DR}} + P_{s,t}^{\mathrm{EV}}\right) - \min_{t=1,\ldots,T}\left(P_{s,t}^{\mathrm{DR}} + P_{s,t}^{\mathrm{EV}}\right)\right)\cdot C^{pun}\cdot\Delta t$	[227]
Annualized capital cost of devices	$C_{\mathrm{ANN}} = \sum_{i=1}^{N} C_{\mathrm{INV}}^{i}\cdot\mathrm{CRF}^{i}$	[228]
Profit of selling electricity to the grid	$C_{\mathrm{SAL}}^{\mathrm{GRID}} = \sum_{m}\sum_{h} d_m\cdot P_{\mathrm{SAL}}^{\mathrm{PV}}\cdot E_{m,h,\mathrm{SAL}}^{\mathrm{PV}} + \sum_{m}\sum_{h} d_m\cdot P_{\mathrm{SAL}}^{\mathrm{CHP}}\cdot E_{m,h,\mathrm{SAL}}^{\mathrm{CHP}}$	[228]
Profit of stepped demand response incentive compensation	$F_{\mathrm{IDR,STP}}^{t} = \begin{cases} \sigma_{\mathrm{IDR}}^{t}\Delta L_{\mathrm{IDR}}^{t}, \Delta L_{\mathrm{IDR}}^{t} < m \\ \sigma_{\mathrm{IDR}}^{t}\left[\Delta L_{\mathrm{IDR}}^{t} + (2-1)\omega\left(\Delta L_{\mathrm{IDR}}^{t} - m\right)\right], m < \Delta L_{\mathrm{IDR}}^{t} < 2m \\ \cdots \\ \sigma_{\mathrm{IDR}}^{t}\left[\begin{array}{c}\Delta L_{\mathrm{IDR}}^{t} + \omega\left(\Delta L_{\mathrm{IDR}}^{t} - m\right) + \ldots \\ +(n-1)\omega\left(\Delta L_{\mathrm{IDR}}^{t} - (n-1)m\right)\end{array}\right] \\ , (n-1)m < \Delta L_{\mathrm{IDR}}^{t} < nm \end{cases}$	[196]
Profit of net value after carbon trading	$C_{t,i}^{\mathrm{CO_2}} = \mu_c\left(CE_t^i - CQ_t^i\right)$	[185]

Furthermore, in the long-term planning for microgrids, some studies incorporate microgrid construction costs into the capacity configuration. The initial investment cost can be represented as follows [227]:

$$C^{\mathrm{INV}} = S^{\mathrm{PV}}\cdot C^{\mathrm{PV}} + N^{\mathrm{WT}}\cdot C^{\mathrm{WT}} + N^{\mathrm{MG}}\cdot C^{\mathrm{MG}} + Cap^{\mathrm{ESS}}\cdot C^{\mathrm{ESS}} + N^{\mathrm{FCF}}\cdot C^{\mathrm{FCF}} + N^{\mathrm{SCF}}\cdot C^{\mathrm{SCF}} \quad (42)$$

where C^{PV} is the investment cost of solar photovoltaic, CNY/m^2; C^{WT} is the investment cost of wind turbine, CNY/kW; C^{DG} is the investment cost of micro generator, CNY/kW; C^{ESS} is the investment cost of energy storage system, CNY/kW·h; C^{FCF} is the investment cost of the fast charging facility, CNY/kW; and C^{SCF} is the investment cost of a slow charging facility, CNY/kW.

(2) Objective for reducing the environmental impact

During the operation of the microgrid, the consumption of fuels inevitably leads to the emission of greenhouse gases and pollutants. The total gas emissions can be expressed as follows [229]:

$$GHG = \sum_{t=1}^{T}\sum_{k=1}^{K}\sum_{i}\delta_{k,i}P_{k,t}^{\mathrm{CDG}} + \sum_{t=1}^{T}\sum_{i}\delta_{\mathrm{UG}_i}P_t^{\mathrm{UG}} \quad (43)$$

where i represents the type of the greenhouse gas pollutant; $\delta_{k,i}$ represents the emission coefficients of gas i in the generator k, g/kW; and δ_{UG_i} represents the gas emission coefficient of grid power, g/kW.

The carbon market is currently highly active, requiring the power system to pay extra penalty charges for carbon dioxide emissions. Therefore, the goal of reducing the environmental impact is often integrated with economic considerations due to the carbon trading mechanism. In addition, if the carbon emission level of an industrial microgrid falls below the allocated quota, the surplus may be used to create economic profit. The carbon tax imposed on the emissions from the power system are presented in Equation (44) [228], respectively.

$$C_{\mathrm{CARBTAX}} = CT \cdot \sum_{i} \sum_{m} \sum_{h} \left[\left(d_m CI_{\mathrm{GAS}} \left(\begin{array}{c} \left(d_m CI_{\mathrm{ELEC}} E_{i,m,h}^{\mathrm{GRID}} \right) + \\ \frac{\left(E_{i,m,h,\mathrm{SELF}}^{\mathrm{CHP}} + E_{i,m,h,\mathrm{SAL}}^{\mathrm{CHP}} + E_{i,m,h,\mathrm{DEL}}^{\mathrm{CHP}} \right)}{\eta_e^{\mathrm{CHP}}} \\ + \frac{H_{i,m,h}^{\mathrm{B}}}{\eta_{\mathrm{th}}^{\mathrm{B}}} \end{array} \right) \right) \right] \tag{44}$$

where CI_{ELEC} represents the carbon intensity of electricity, $\mathrm{kgCO_2/kWh}$; CI_{GAS} represents the carbon intensity of natural gas, $\mathrm{kg\text{-}CO_2/kWh}$; d_m represents the number of days in every month; $E_{i,m,h}^{\mathrm{GRID}}$ represents the monthly average of purchased electricity from the grid at month m hour h, kW; and $H_{i,m,h}^{\mathrm{B}}$ represents the monthly average of generated heat by the boiler at month m hour h, kW.

The carbon emission allowance can be calculated by the following [230]:

$$C_{\mathrm{sys,c}} = \eta_{\mathrm{cq}} \sum_{i=1}^{T} \left[\sum_{i=1}^{P} \varphi P_{\mathrm{GT},i,t} + \sum_{i=1}^{Q} P_{\mathrm{GB},i,t} \right] \tag{45}$$

where η_{cq} represents the carbon quota coefficient of gas turbine and gas boiler, φ represents the electric-heat conversion coefficient of gas turbine, and $P_{\mathrm{GT},i,t}$ and $P_{\mathrm{GB},i,t}$ represent the output power of the gas turbine and gas boiler, respectively.

(3) Objective for improving users' satisfaction

User satisfaction is also crucial for measuring the operation of microgrids, reflecting the comprehensive performance of microgrids in meeting users' load demands, ensuring power supply stability, enhancing sustainability, and reducing the economic cost. The common objective function for maximizing users' satisfaction under different considerations of energy costs, energy utilization comfort, interruptible loads, and the integration of renewable energy is formulated as follows [224,230–234].

$$\max R_{\mathrm{exp}} = 1 - \frac{\sum_{t=1}^{T} |\pi_t^* P_t^* - \pi_t P_t|}{\sum_{t=1}^{T} \pi_t P_t} \tag{46}$$

$$\max R_{\mathrm{com}} = 1 - \frac{\sum_{t=1}^{T} |P_t - P_t^*|}{\sum_{t=1}^{T} P_t} \tag{47}$$

$$\max R_{\mathrm{loss}} = 1 - \vartheta_i \frac{\Delta P_{\mathrm{load}} \times R_{\mathrm{sl}}}{P_{\mathrm{load}} \pi} \tag{48}$$

$$\max R_{\mathrm{RWE}} = \frac{\sum_{t=1}^{T} (P_{\mathrm{RWE},t} - P_{\mathrm{A-RWE},t})}{\sum_{t=1}^{T} P_{\mathrm{RWE},t}} \tag{49}$$

where R_{exp} represents the level of satisfaction with electricity spending, R_{com} represents the degree of comfort with energy usage, R_{loss} represents the users' satisfaction with an interruptible load, R_{sl} represents the subsidy to compensate for the power shortage loss after the demand response, π_t and π_t^* represent the time-of-use price before and after demand response, and R_{RWE} represents the level of microgrids' integration with renewable energy.

(4) Objective for reducing the operational risk

The risks arising from uncertainties in the power supply, reliability issues, economic factors, and operational failures pose significant challenges to the economical and rational operation of microgrids. Consequently, risk management has become a critical factor that microgrid operators must consider [235]. For example, Chen et al. [234] proposed a risk measurement method based on credibility theory, which comprehensively evaluates uncertain wind power from both stochastic and fuzzy perspectives. Anam et al. [236] proposed a risk-based resilient microgrid-optimization method, which enhances system resilience through a fault-driven method and strengthens survivability by either prioritizing or curtailing critical loads. By implementing proactive control in advance, microgrids can enhance their adaptability to uncertainties and effectively mitigate operational risks.

(5) Multi-objective optimization

Moreover, multi-objective optimization methods are often employed in the scheduling process to achieve the optimal trade-off among multiple metrics. Membership functions are used in some studies to weigh and balance multiple objectives [237,238]. Algorithms such as MOPSO, PESA II, NSGA, and SPEA2 are employed to identify optimal solutions based on their specific mechanisms [239]. In addition, the utilization of Pareto optimization in multi-objective problems enables the optimal trade-off between multiple indicators. Pareto introduces the concept of non-dominance, where the optimal solution cannot be improved in any objective without deteriorating another.

5.4.2. Constraint Conditions

Some constraint conditions should be thoroughly considered to regulate the operational behavior of microgrids in the construction of a simulation model:

(1) Constraint on power balance

$$\sum_{i=1} P_{\mathrm{EG},i}(t) + P_{\mathrm{grid}}(t) + P_{\mathrm{ES}}(t) = P_{\mathrm{load}}(t) \tag{50}$$

where $P_{\mathrm{EG},i}(t)$ represents the output of generation facility i at time t, which includes photovoltaic, wind power, fuel cells, and distributed micro turbines; $P_{\mathrm{grid}}(t)$ represents the power exchange between microgrid and grid at time t, which can involve either selling or purchasing electricity (the transmission power between the distribution network and the microgrid); $P_{\mathrm{ES}}(t)$ represents the charging or discharging power of the energy storage unit at time t (a positive value indicates discharging and a negative value indicates charging); and $P_{\mathrm{load}}(t)$ denotes the load demand at time t.

(2) Constraint on power-generation units

The power-generation capacity constraint of each scheduling unit, the constraint of power exchanged between microgrid and grid, and the charging and discharging power constraints of energy storage can be expressed by Equations (51)–(54), respectively [192]:

$$P_{\mathrm{MIN,EG},i} \le P_{\mathrm{EG},i}(t) \le P_{\mathrm{MAX,EG},i} \tag{51}$$

$$P_{\mathrm{min,grid}} \le P_{\mathrm{grid}}(t) \le P_{\mathrm{max,grid}} \tag{52}$$

$$P_{\mathrm{MIN,ES,ch}} \le P_{\mathrm{ES,ch}}(t) \le P_{\mathrm{MAX,ES,ch}} \tag{53}$$

$$P_{\mathrm{MIN,ES,dis}} \le P_{\mathrm{ES,dis}}(t) \le P_{\mathrm{MAX,ES,dis}} \tag{54}$$

where MIN represents the minimum output limit of the components; MAX represents the maximum output limit of the components.

The ramp rate refers to the increase or decrease in the output power of distributed generation within a unit of time. For example, the ramping constraint of a gas turbine can be expressed as follows [240]:

$$-R_{\mathrm{d}}\Delta t \le P_{\mathrm{EG,MT}}(t) - P_{\mathrm{EG,MT}}(t-\Delta t)\Delta R_{\mathrm{u}}\Delta t \tag{55}$$

where $P_{\mathrm{EG,MT}}(t)$ represents the output power of the micro gas turbine; R_{d} and R_{u} denote the downward and upward ramp rates of the micro gas turbine, respectively.

(3) Constraint on components' capacity.

The capacity constraints of the battery can be expressed as follows:

$$SOC_{\mathrm{MIN}} \le SOC_{\mathrm{BT}}(t) \le SOC_{\mathrm{MAX}} \tag{56}$$

where $SOC_{\mathrm{BT}}(t)$ represents the state of charge; SOC_{MIN} and SOC_{MAX} represent the lower and upper capacity limits of the battery, respectively.

The capacity constraint of the hydrogen storage tank can be expressed as follows:

$$C_{\mathrm{MIN,HS}} \le C_{\mathrm{HS}}(t) \le C_{\mathrm{MAX,HS}} \tag{57}$$

where $C_{\mathrm{HS}}(t)$ represents the hydrogen storage state; $C_{\mathrm{MIN,HS}}$ and $C_{\mathrm{MAX,HS}}$ represent the lower and upper limits of the hydrogen storage capacity, respectively.

(4) Constraint on operating conditions

The constraints on the charging and discharging state for the battery or hydrogen storage can be expressed by the following:

$$\mu_{\mathrm{ch}(t)} + \mu_{\mathrm{dis}(t)} \le 1 \tag{58}$$

where $\mu_{\mathrm{ch}(t)}$ and $\mu_{\mathrm{dis}(t)}$ are binary variables representing the charging and discharging states.

To maintain the autonomy of the microgrid, the import of energy from the external grid should be restricted within a reasonable range [184].

$$1 - \sum_{s=1}^{S}\sum_{t=1}^{T}\left[\frac{P_{\mathrm{PG},t}^{s}}{L_{t}^{\mathrm{power},s}}\right] \ge \Phi_{\mathrm{PG}} \tag{59}$$

where Φ_{PG} represents the minimum self-sufficiency ratio for power, $P_{\mathrm{PG},t}^{s}$ refers to the imported external energy, and $L_{t}^{\mathrm{power},s}$ represents the power load at time t.

The constraints on daily start–stop cycles of the generator unit can be expressed as follows:

$$\sum_{t=0}^{T}|\mu_{t+1} - \mu_{t}| \le N_{\max} \tag{60}$$

where μ_{t+1} and μ_{t} are binary variables representing the operational status of the equipment at adjacent time periods; $N_{\max}$ represents the maximum number of the start–stop cycle.

(5) Constraint on the demand response

To prevent peak–valley fluctuations in the load, the adjustment limits of the demand response are as follows [184]:

$$\begin{cases} \left|\Delta L_{\mathrm{PB},t}^{z}\right| \le \Delta L_{t}^{z,\max} \\ \sum\limits_{t=1}^{T}\Delta L_{\mathrm{PB},t}^{z} \le \Delta L_{\mathrm{total}}^{\max} \end{cases} \tag{61}$$

$$\begin{cases} \Delta L_{\mathrm{IB},t}^{z,\min} \le \Delta L_{\mathrm{IB},t}^{z} \le \Delta L_{\mathrm{IB},t}^{z,\max} \\ \Delta L_{\mathrm{IB},k,t}^{z,u,\min} \le \Delta L_{\mathrm{IB},k,t}^{z,u} - \Delta L_{\mathrm{IB},k,t-1}^{z,u} \le \Delta L_{\mathrm{IB},k,t}^{z,u,\max} \\ \Delta L_{\mathrm{IB},k,t}^{z,d,\min} \le \Delta L_{\mathrm{IB},k,t}^{z,d} - \Delta L_{\mathrm{IB},k,t-1}^{z,d} \le \Delta L_{\mathrm{IB},k,t}^{z,d,\max} \end{cases} \tag{62}$$

where $\Delta L_{t}^{z,\max}$ and $\Delta L_{\mathrm{total}}^{\max}$ represent the maximum instantaneous load adjustment per interval and cumulative adjustment limit over the scheduling period; $\Delta L_{\mathrm{IB},t}^{z,\max}$, $\Delta L_{\mathrm{IB},k,t}^{z,u,\max}$ and $\Delta L_{\mathrm{IB},k,t}^{z,d,\max}$ represent the cumulative adjustment limit over the scheduling period and the maximum increase or decrease adjustment per interval.

The flexible load should satisfy the following constraints [196]:

$$\frac{L_{\mathrm{shift,out}}^{k,t}}{L_{\mathrm{base}}^{k,t} + \overline{L}_{\mathrm{shift}}^{k,t} + \overline{L}_{\mathrm{cut}}^{k,t}} \le \alpha \tag{63}$$

$$\frac{L_{\mathrm{cut}}^{k,t}}{L_{\mathrm{base}}^{k,t} + \overline{L}_{\mathrm{shift}}^{k,t} + \overline{L}_{\mathrm{cut}}^{k,t}} \le \beta \tag{64}$$

$$\sum_{t=1}^{T} L_{\mathrm{shift}}^{k,t} = 0 \tag{65}$$

where L_{base}^{t} represents the base load at time t; $\overline{L}_{\mathrm{shift}}^{k,t}$ and $\overline{L}_{\mathrm{cut}}^{k,t}$ represent the shiftable and curtailable loads prior to demand response at time t, respectively.

6. Key Issues and Future Directions in Modeling of Industrial Microgrid

Integrating renewable energy is a crucial step toward achieving industrial carbon peaking, which makes efficient energy management a top priority. Currently, significant attention has been given to research challenges in areas such as microgrid planning, regulation, and evaluation. However, several critical issues remain in both current and future research on industrial microgrids, which require ongoing attention and resolution.

(1) Reliability challenge. Industrial loads often have stringent power quality requirements and require a continuous and stable power supply. The frequent power fluctuations can cause production disruptions or equipment damage, which poses new demands on the control technology and fault tolerance of the industrial microgrids. The power sources, energy storage devices, and industrial loads are expected to function as plug-and-play units, which will significantly increase the complexity of system scheduling and control [29,241]. Therefore, more precise and advanced modeling methods for forecasting and scheduling to redesign the microgrid system need to be developed.

(2) Economics challenge. Although microgrids are technically mature, the construction of the microgrid infrastructure, including crucial components such as energy storage, still faces high investment costs. The economic benefits are clearly insufficient in the short term, making them economically unfeasible [242]. Therefore, the application of microgrid technology in traditional industrial sectors will not be accepted at once due to the increased financial burden. It is necessary to develop microgrid models that fully integrate market mechanisms and cost optimization to explore the patterns of cost control and profit gain suitable for the industrial sector [243].

(3) Market challenge. The industrial microgrids inevitably interact with the grid due to the uncertainty of source and load. In order to further generate profits and recover economic costs, industrial microgrids may need to engage in the power ancillary services market. Three patterns have been proposed for integrating energy prosumers into the grid: peer-to-peer, prosumer-to-grid, and prosumer community groups, which exhibit different operational mechanisms and barriers [243]. Microgrids still face numerous challenges in the process of marketization. An appropriate market

infrastructure should be established and implemented, along with the continuous development of innovative business models, in order to effectively support the long-term development of industrial microgrids.

(4) Multi-energy coupling. Compared to independent power grids, industrial sectors often involve multiple energy carriers, leading to more complex energy flows. The traditional optimization methods struggle to handle the complex coupling relationships among multiple energy mediums, requiring more precise models to accurately depict the energy interactions and metabolic processes of multi-energy industrial systems.

(5) Data management. The data acquisition, management, and disclosure level of some industrial enterprises are relatively inadequate, which may lead to data barriers between multiple entities during microgrid operation. The collection of power load data is often too coarse in terms of time granularity and is frequently biased in current energy management and control systems of industrial enterprises, severely affecting the precise optimization and scheduling of microgrids. Consequently, a more robust and unified data-management architecture needs to be established.

7. Conclusions

The advancement of innovative renewable energy and grid technologies has introduced new paradigms and methodologies for industrial energy management. Particularly under the vision of Industry 5.0, the commercialization of microgrids remains sluggish, necessitating intelligent and digital transformation for their effective implementation. The application of industrial big data, the construction of intelligent management platforms, and core computational models have emerged as critical components. A knowledge framework for energy scheduling and management modeling centered on industrial microgrids, providing prior knowledge on microgrid modeling, has been established to support its industrial deployment. The fundamental concepts and architecture of industrial microgrids are elucidated, encompassing renewable energy sources, energy storage systems, control mechanisms, and communication infrastructures. The reliable source-load forecasting technologies serve as the foundation for efficient microgrid scheduling by offering robust data support. This review presents a comprehensive forecasting framework, including data preprocessing, forecasting strategies, predictive modeling, and model evaluation. As the big data, artificial intelligence, and communication technologies continue to perform integrated development, the accuracy and real-time capability of power and load forecasting will be further enhanced. The scheduling function serves as the central component of modern microgrids, aiming to optimize power distribution, maintain the supply–demand balance, regulate power stability, and improve the economic performance of the system. This study develops a modeling framework for intelligent optimization and scheduling in microgrids, providing a comprehensive summary and analysis from multiple perspectives, including fundamental physical component modeling, scheduling rules and strategies, optimization objectives, and multiple constraints. Highly efficient optimization strategies and frameworks are essential to facilitate optimal decision-making in microgrid operations. The future research works will address challenges related to the economic viability, stability, market integration, and operational management of microgrids, continuously exploring innovative paradigms for industrial microgrid applications.

Author Contributions: L.Z.: Conceptualization, Methodology, Writing—original draft. Y.Y.: Methodology, Visualization. S.Y.: Formal analysis, Investigation. H.C.: Software. T.D.: Supervision, Project administration, Writing—review and editing. All authors have read and agreed to the published version of the manuscript.

Funding: The authors are grateful to the financial support provided by National Natural Science Foundation of China (No.: U24A20195, No.: 52270177), Young Elite Scientists Sponsorship Program by CAST (No.: 2022QNRC001), Doctoral Research Initiation Fund Program in Liaoning Province (No.: 2023-BS-054), the 111 Project (B16009), and the Key Technical Research Project of Shenyang (No. 22-101-0-28).

Data Availability Statement: The original contributions presented in the study are included in the article, further inquiries can be directed to the corresponding author.

Conflicts of Interest: The authors declare that they have no known competing financial interests or personal relationships that could have appeared to influence the work reported in this paper.

Appendix A

Table A1. Basic information of different energy storage methods.

Categories	Storage Methods	Energy Density Wh/kg	Power Density W/kg	Response Time	Discharge	Efficiency %	Cycling Capability	Lifetime Year	Cost	Refs.
Mechanical energy storage	Flywheel energy storage	5–130	200–500	s-min	ms-40 min	85–90	10^5–10^7	20	400–800 $/kWh	[47,244–247]
	Pump hydro energy storage	0.5–1.5		ms-s	1–24 h	65–87	2×10^4–5×10^4	30–50	10–70 €/kWh	[245–248]
	Compressed air energy storage	30–60		1–15 min	1–24 h	70–80		20–60	10–120 €/kWh	[47,246,247]
Electromagnetic energy storage	Superconducting magnetic energy storage	0.1–15	500–2000	<100 ms	ms-min	80–95	10^4–10^5	20	8974 €/kWh	[47,245–247]
	Super capacitor	1–15	500–2000		10–30	85–95		20	1795 €/kWh	[47,244,249]
Electrochemical energy storage	Lithium-ion battery	80–150	245–500	20 ms-s	1 min–1 h	78–88	1500–3500	14–16	900–1300 $/kWh	[47,245,247]
	Lead-acid battery	30–50	180–200	5–10 ms	1 s–1 h	75–80	200–500	15	50–100 €/kWh	[245,247]
	Nickel cadmium battery	30–50	100–160	20 ms-s	1 s–1 h	72	3500	13–20	400–2400 $/kWh	[245,247]
	Sodium sulfur battery	100–175	115–230	ms, s	1 s–1 h	75–87	2500	12–20	210–450 €/kWh	[245–247,250]
	Flow battery	20–70	-	10 s	1 s–1 h	60–70	10^4	10–15	150–1000 $/kWh	[47,247,249]
Thermal energy storage	Sensible heat storage	10–120	-	-	-	50–90	-	-	0.1–10 €/kWh	[249,251]
	Latent heat storage	150–250	-	-	-	75–90	-	--	10–50 €/kWh	[47,249,251]
	Thermochemical energy storage	120–250	-	-	-	75–100	-	-	8–100 €/kWh	[251]
Chemical energy storage	Hydrogen energy storage	800–10,000	-	-	-	35–42	2×10^4	15	12–15 €/kWh	[245,249]

Table A2. Scheduling strategies and rules of microgrids.

Strategies	Refs.
Renewable energy is prioritized for consumption in microgrids. Electrical loads are classified into peak, flat, and off-peak periods to establish time-of-use pricing and guide electricity consumption behavior.	Qiao et al. [252]
The real-time price of electricity is used to optimize the charging and discharging strategies of electric vehicles.	Mei et al. [192]
Renewable energy generation is prioritized to be consumed locally and meet load demands. Surplus power is used to charge shared storage, and the remaining electricity is sold to the grid. When the microgrid is unable to meet load demands, stored energy is used first, followed by purchasing from the grid. The allocation strategy is formulated based on transaction prices and investment proportions.	Dai et al. [253]
A real-time electricity pricing strategy combining the reward and penalty for reactive power is proposed.	Fang et al. [254]
The RA model is utilized to minimize risk under the worst-case deviation of uncertain wind power variables from their predicted values, while the RS model aims to maximize wind power capacity under the condition of minimized uncertainty fluctuations.	Xiao et al. [255]
By incorporating dynamic pricing, interactive power with the grid, and the dispatchability of electric vehicles, the microgrid can serve as a user to participate in peak shaving ancillary services. During periods of high power demand, surplus electricity can be sold to the ancillary services market as a peak-shaving resource.	Huang et al. [256]
Scheduling based on risk management; multi-energy microgrids participate in the electricity, natural gas, and hydrogen energy markets three days in advance to procure a significant portion of the required energy.	Salyani et al. [257]
Shared energy storage of microgrid groups. SESO issues rental prices to MGCO, which responds to the price signals and obtains the final scheduling plan after repeated allocation.	Qiao et al. [258]
Peak pricing imposes higher rates during periods of extreme demand, thereby incentivizing reduced consumption during these times. Real-time pricing offers prices that fluctuate in real-time according to current market conditions, providing the fastest response pricing scheme.	Rochd et al. [259]
A non-cooperative Stackelberg game relationship is formed among the participants of the microgrid system.	Zhao et al. [260]
A price-based demand response strategy is used to construct the energy-management model of the microgrid system, and a novel charging and discharging strategy for the microgrid system is proposed.	Li et al. [261]
Based on the real-time feedback information of the system (such as load demand, renewable energy output power, energy storage status, etc.), priority is given to uncontrollable power sources and the energy storage capacity, and corresponding decisions can be made during the power scheduling process.	Wu et al. [198]

Table A2. *Cont.*

Strategies	Refs.
The operator responds to price signals by shifting flexible loads from peak periods to off-peak periods. Electricity price information is transmitted through the microgrid operator, including the purchase price from the day-ahead market and the purchase and sale prices from the real-time market.	Guo et al. [16]
A dynamic leader–follower game with multiple stakeholders.	Yang et al. [262]
Minimize the community-microgrid cost through the prioritized selection of participants for demand reduction. A novel decentralized three non-cooperative dynamic games strategy is proposed, incorporating Nash equilibrium approaches to achieve the optimum schedules of appliance, buying, and power trading agents to maximize the net present value of both prosumers and the community-microgrid.	Hussain et al. [263]

Table A3. Comparison of the performance of common algorithms.

Algorithm	Accuracy/%	MAE	RMSE	Refs.
Random forest	91.32	0.0124	0.0169	[264–266]
Logistic regression	91.32	0.8800	0.25	[164,265,266]
Support Vector Regression	85.11	0.8520	0.17	[164,265,266]
Decision tree	40.78	0.7600	-	[265]
K-nearest neighbors	80.15	0.0108	0.0258	[264,266]
Naïve Bayes	84.86	0.0940	0.2230	[266]
LSTM	-	0.0117	0.0145	[165]
MLP	-	0.0464	0.0589	[165]
Linear regression	-	0.8800	-	[265]
ANN	92.80	0.0420	0.1500	[266]

References

1. Peng, K.; Feng, K.; Chen, B.; Shan, Y.; Zhang, N.; Wang, P.; Fang, K.; Bai, Y.; Zou, X.; Wei, W.; et al. The global power sector's low-carbon transition may enhance sustainable development goal achievement. *Nat. Commun.* **2023**, *14*, 3144. [CrossRef] [PubMed]
2. Xie, X.; Fu, H.; Zhu, Q.; Hu, S. Integrated optimization modelling framework for low-carbon and green regional transitions through resource-based industrial symbiosis. *Nat. Commun.* **2024**, *15*, 3842. [CrossRef] [PubMed]
3. Huang, M.-T.; Zhai, P.-M. Achieving Paris Agreement temperature goals requires carbon neutrality by middle century with far-reaching transitions in the whole society. *Adv. Clim. Change Res.* **2021**, *12*, 281–286. [CrossRef]
4. He, K.; Wang, L. A review of energy use and energy-efficient technologies for the iron and steel industry. *Renew. Sustain. Energy Rev.* **2017**, *70*, 1022–1039. [CrossRef]
5. Yu, B.; Fang, D.; Xiao, K.; Pan, Y. Drivers of renewable energy penetration and its role in power sector's deep decarbonization towards carbon peak. *Renew. Sustain. Energy Rev.* **2023**, *178*, 113247. [CrossRef]
6. Ryu, H.; Dorjragchaa, S.; Kim, Y.; Kim, K. Electricity-generation mix considering energy security and carbon emission mitigation: Case of Korea and Mongolia. *Energy* **2014**, *64*, 1071–1079. [CrossRef]
7. Saeed, M.H.; Fangzong, W.; Kalwar, B.A.; Iqbal, S. A review on microgrids' challenges & perspectives. *IEEE Access* **2021**, *9*, 166502–166517. [CrossRef]
8. Alasali, F.; Saad, S.M.; Saidi, A.S.; Itradat, A.; Holderbaum, W.; El-Naily, N.; Elkuwafi, F.F. Powering up microgrids: A comprehensive review of innovative and intelligent protection approaches for enhanced reliability. *Energy Rep.* **2023**, *10*, 1899–1924. [CrossRef]
9. Pullins, S. Why microgrids are becoming an important part of the energy infrastructure. *Electr. J.* **2019**, *32*, 17–21. [CrossRef]
10. Abbasi, M.; Abbasi, E.; Li, L.; Aguilera, R.P.; Lu, D.; Wang, F. Review on the microgrid concept, structures, components, communication systems, and control methods. *Energies* **2023**, *16*, 484. [CrossRef]
11. Shahzad, S.; Abbasi, M.A.; Ali, H.; Iqbal, M.; Munir, R.; Kilic, H. Possibilities, challenges, and future opportunities of microgrids: A review. *Sustainability* **2023**, *15*, 6366. [CrossRef]
12. Agha Kassab, F.; Rodriguez, R.; Celik, B.; Locment, F.; Sechilariu, M. A Comprehensive review of sizing and energy management strategies for optimal planning of microgrids with PV and other renewable integration. *Appl. Sci.* **2024**, *14*, 10479. [CrossRef]
13. Blake, S.T.; Sullivan, D.T.J. Optimization of distributed energy resources in an Industrial Microgrid. *Procedia CIRP* **2018**, *67*, 104–109. [CrossRef]
14. Li, J.H.; Zhong, J.X.; Wang, K.L.; Luo, Y.; Han, Q.; Tan, J.R. Research on multi-objective optimization model of industrial microgrid considering demand response technology and user satisfaction. *Energy Eng.* **2023**, *120*, 869–884. [CrossRef]
15. Misaghian, M.S.; Saffari, M.; Kia, M.; Heidari, A.; Shafie-khah, M.; Catalao, J.P.S. Tri-level optimization of industrial microgrids considering renewable energy sources, combined heat and power units, thermal and electrical storage systems. *Energy* **2018**, *161*, 396–411. [CrossRef]
16. Guo, S.L.; He, J.Q.; Ma, K.; Yang, J.; Wang, Y.C.; Li, P.P. Robust economic dispatch for industrial microgrids with electric vehicle demand response. *Renew. Energy* **2025**, *240*, 122210. [CrossRef]
17. Daneshvar, M.; Eskandari, H.; Sirous, A.B.; Esmaeilzadeh, R. A novel techno-economic risk-averse strategy for optimal scheduling of renewable-based industrial microgrid. *Sustain. Cities Soc.* **2021**, *70*, 102879. [CrossRef]

18. Feng, W.; Jin, M.; Liu, X.; Bao, Y.; Marnay, C.; Yao, C.; Yu, J. A review of microgrid development in the United States—A decade of progress on policies, demonstrations, controls, and software tools. *Appl. Energy* **2018**, *228*, 1656–1668. [CrossRef]
19. Qu, M.; Ding, T.; Huang, L.; Wu, X. Toward a Global Green Smart Microgrid: An Industrial Park in China. *IEEE Electrif. Mag.* **2020**, *8*, 55–69. [CrossRef]
20. Cetinkaya, H.B.; Kucuk, S.; Unaldi, M.; Gokce, G.B. A case study of a successful industrial microgrid operation. In Proceedings of the 2017 4th International Conference on Electrical and Electronic Engineering (ICEEE), Ankara, Turkey, 8–10 April 2017; pp. 95–98. [CrossRef]
21. Yuan, Y.; Na, H.; Chen, C.; Qiu, Z.; Sun, J.; Zhang, L.; Du, T.; Yang, Y. Status, challenges, and prospects of energy efficiency improvement methods in steel production: A multi-perspective review. *Energy* **2024**, *304*, 132047. [CrossRef]
22. Na, H.; Qiu, Z.; Sun, J.; Yuan, Y.; Zhang, L.; Du, T. Revealing cradle-to-gate CO2 emissions for steel product producing by different technological pathways based on material flow analysis. *Resour. Conserv. Recycl.* **2024**, *203*, 107416. [CrossRef]
23. Ottenburger, S.S.; Cox, R.; Chowdhury, B.H.; Trybushnyi, D.; Al Omar, E.; Kaloti, S.A.; Ufer, U.; Poganietz, W.-R.; Liu, W.; Deines, E.; et al. Sustainable urban transformations based on integrated microgrid designs. *Nat. Sustain.* **2024**, *7*, 1067–1079. [CrossRef]
24. Qamar, H.G.M.; Guo, X.; Ahmad, F. Intelligent energy management system of hydrogen based microgrid empowered by AI optimization technique. *Renew. Energy* **2024**, *237*, 121738. [CrossRef]
25. Chaouachi, A.; Kamel, R.M.; Andoulsi, R.; Nagasaka, K. Multiobjective intelligent energy management for a microgrid. *IEEE Trans. Ind. Electron.* **2013**, *60*, 1688–1699. [CrossRef]
26. Monchusi, B.B. A comprehensive review of microgrid technologies and applications. In Proceedings of the 2023 International Conference on Electrical, Computer and Energy Technologies (ICECET), Cape Town, South Africa, 16–17 November 2023; pp. 1–7. [CrossRef]
27. Sang, J.; Sun, H.; Kou, L. Deep reinforcement learning microgrid optimization strategy considering priority flexible demand side. *Sensors* **2022**, *22*, 2256. [CrossRef]
28. Su, Y. Smart energy for smart built environment: A review for combined objectives of affordable sustainable green. *Sustain. Cities Soc.* **2020**, *53*, 101954. [CrossRef]
29. Uddin, M.; Mo, H.; Dong, D.; Elsawah, S.; Zhu, J.; Guerrero, J.M. Microgrids: A review, outstanding issues and future trends. *Energy Strategy Rev.* **2023**, *49*, 101127. [CrossRef]
30. Yoldaş, Y.; Önen, A.; Muyeen, S.M.; Vasilakos, A.V.; Alan, İ. Enhancing smart grid with microgrids: Challenges and opportunities. *Renew. Sustain. Energy Rev.* **2017**, *72*, 205–214. [CrossRef]
31. Kakran, S.; Chanana, S. Smart operations of smart grids integrated with distributed generation: A review. *Renew. Sustain. Energy Rev.* **2018**, *81*, 524–535. [CrossRef]
32. Cagnano, A.; De Tuglie, E.; Mancarella, P. Microgrids: Overview and guidelines for practical implementations and operation. *Appl. Energy* **2020**, *258*, 114039. [CrossRef]
33. Moharm, K. State of the art in big data applications in microgrid: A review. *Adv. Eng. Inform.* **2019**, *42*, 100945. [CrossRef]
34. Zhou, K.; Fu, C.; Yang, S. Big data driven smart energy management: From big data to big insights. *Renew. Sustain. Energy Rev.* **2016**, *56*, 215–225. [CrossRef]
35. Silva, C.; Faria, P.; Vale, Z.; Corchado, J.M. Demand response performance and uncertainty: A systematic literature review. *Energy Strategy Rev.* **2022**, *41*, 100857. [CrossRef]
36. Patteeuw, D.; Bruninx, K.; Arteconi, A.; Delarue, E.; D'haeseleer, W.; Helsen, L. Integrated modeling of active demand response with electric heating systems coupled to thermal energy storage systems. *Appl. Energy* **2015**, *151*, 306–319. [CrossRef]
37. Wang, Z.; Gu, C.; Li, F.; Bale, P.; Sun, H. Active Demand Response Using Shared Energy Storage for Household Energy Management. *IEEE Trans. Smart Grid* **2013**, *4*, 1888–1897. [CrossRef]
38. Lu, R.; Hong, S.H. Incentive-based demand response for smart grid with reinforcement learning and deep neural network. *Appl. Energy* **2019**, *236*, 937–949. [CrossRef]
39. Dutta, O.; Mohamed, A. Community microgrid: Control structure, design, and stability. *Fuel Commun.* **2024**, *18*, 100105. [CrossRef]
40. Kanakadhurga, D.; Prabaharan, N. Demand side management in microgrid: A critical review of key issues and recent trends. *Renew. Sustain. Energy Rev.* **2022**, *156*, 111915. [CrossRef]
41. Mah, A.X.Y.; Ho, W.S.; Hassim, M.H.; Hashim, H.; Ling, G.H.T.; Ho, C.S.; Ab Muis, Z. Optimization of a standalone photovoltaic-based microgrid with electrical and hydrogen loads. *Energy* **2021**, *235*, 121218. [CrossRef]
42. Duan, F.; Eslami, M.; Khajehzadeh, M.; Basem, A.; Jasim, D.J.; Palani, S. Optimization of a photovoltaic/wind/battery energy-based microgrid in distribution network using machine learning and fuzzy multi-objective improved Kepler optimizer algorithms. *Sci. Rep.* **2024**, *14*, 13354. [CrossRef]
43. Bacha, S.; Picault, D.; Burger, B.; Etxeberria-Otadui, I.; Martins, J. Photovoltaics in Microgrids: An Overview of Grid Integration and Energy Management Aspects. *IEEE Ind. Electron. Mag.* **2015**, *9*, 33–46. [CrossRef]
44. Zheng, Y.; Jenkins, B.M.; Kornbluth, K.; Kendall, A.; Træholt, C. Optimization of a biomass-integrated renewable energy microgrid with demand side management under uncertainty. *Appl. Energy* **2018**, *230*, 836–844. [CrossRef]

45. Tariq, A.H.; Kazmi, S.A.A.; Hassan, M.; Muhammed Ali, S.A.; Anwar, M. Analysis of fuel cell integration with hybrid microgrid systems for clean energy: A comparative review. *Int. J. Hydrog. Energy* **2024**, *52*, 1005–1034. [CrossRef]
46. Halev, A.; Liu, Y.; Liu, X. Microgrid control under uncertainty. *Eng. Appl. Artif. Intell.* **2024**, *138*, 109360. [CrossRef]
47. Elalfy, D.A.; Gouda, E.; Kotb, M.F.; Bureš, V.; Sedhom, B.E. Comprehensive review of energy storage systems technologies, objectives, challenges, and future trends. *Energy Strategy Rev.* **2024**, *54*, 101482. [CrossRef]
48. Baimel, D.; Tapuchi, S.; Baimel, N. Smart grid communication technologies- overview, research challenges and opportunities. In Proceedings of the 2016 International Symposium on Power Electronics, Electrical Drives, Automation and Motion (SPEEDAM), Capri, Italy, 22–24 June 2016; pp. 116–120. [CrossRef]
49. Serban, I.; Céspedes, S.; Marinescu, C.; Azurdia-Meza, C.A.; Gómez, J.S.; Hueichapan, D.S. Communication Requirements in Microgrids: A Practical Survey. *IEEE Access* **2020**, *8*, 47694–47712. [CrossRef]
50. Starke, M.; Herron, A.; King, D.; Xue, Y. Implementation of a publish-subscribe protocol in microgrid islanding and resynchronization with self-discovery. *IEEE Trans. Smart Grid* **2019**, *10*, 361–370. [CrossRef]
51. Bhatt, J.; Harish, V.S.K.V.; Jani, O.; Saini, G. Performance based optimal selection of communication technologies for different smart microgrid applications. *Sustain. Energy Technol. Assess.* **2022**, *53*, 102495. [CrossRef]
52. Reddy, G.P.; Kumar, Y.V.P.; Chakravarthi, M.K. Communication technologies for interoperable smart microgrids in urban energy community: A broad review of the state of the art, challenges, and research perspectives. *Sensors* **2022**, *22*, 5881. [CrossRef]
53. Olivares, D.E.; Mehrizi-Sani, A.; Etemadi, A.H.; Canizares, C.A.; Iravani, R.; Kazerani, M.; Hajimiragha, A.H.; Gomis-Bellmunt, O.; Saeedifard, M.; Palma-Behnke, R.; et al. Trends in microgrid control. *IEEE Trans. Smart Grid* **2014**, *5*, 1905–1919. [CrossRef]
54. Satapathy, A.S.; Mohanty, S.; Mohanty, A.; Rajamony, R.K.; Soudagar, M.E.M.; Khan, T.Y.; Kalam, M.; Ali, M.M.; Bashir, M.N. Emerging technologies, opportunities and challenges for microgrid stability and control. *Energy Rep.* **2024**, *11*, 3562–3580. [CrossRef]
55. Modu, B.; Abdullah, M.P.; Sanusi, M.A.; Hamza, M.F. DC-based microgrid: Topologies, control schemes, and implementations. *Alex. Eng. J.* **2023**, *70*, 61–92. [CrossRef]
56. Arif, M.S.B.; Hasan, M.A. Microgrid architecture, control, and operation. In *Hybrid-Renewable Energy Systems in Microgrids*; Elsevier: Amsterdam, The Netherlands, 2018; pp. 23–37. [CrossRef]
57. Elsayed, A.T.; Mohamed, A.A.; Mohammed, O.A. DC microgrids and distribution systems: An overview. *Electr. Power Syst. Res.* **2015**, *119*, 407–417. [CrossRef]
58. Alam, S.; Hossain, A.; Shafiullah; Islam, A.; Choudhury, M.; Faruque, O.; Abido, M.A. Renewable energy integration with DC microgrids: Challenges and opportunities. *Electr. Power Syst. Res.* **2024**, *234*, 110548. [CrossRef]
59. Ferahtia, S.; Houari, A.; Cioara, T.; Bouznit, M.; Rezk, H.; Djerioui, A. Recent advances on energy management and control of direct current microgrid for smart cities and industry: A Survey. *Appl. Energy* **2024**, *368*, 123501. [CrossRef]
60. Fuhrlaender, D.; Vermeulen, B.; Schnuelle, C. Green hydrogen transformation of the iron and steel production system: An integrated operating concept for system-internal balance, lower emissions, and support for power system stability. *Appl. Energy* **2025**, *381*, 125104. [CrossRef]
61. Wang, P.T.; Xu, Q.C.; Wang, F.Y.; Xu, M. Study on the coupling of the iron and steel industry with renewable energy for low-carbon production: A case study of matching steel plants with photovoltaic power plants in China. *Energy* **2025**, *320*, 135381. [CrossRef]
62. Zhang, L.; Yuan, Y.; Xi, J.; Sun, J.; Yan, S.; Du, T.; Na, H. Synergistic enhancement for energy-saving, emission reduction and profit improvement in iron and steel manufacturing system: Strategies for parameter regulation and technologies integration. *Energy Convers. Manag.* **2024**, *322*, 119101. [CrossRef]
63. Zhang, L.; Na, H.; Yuan, Y.; Sun, J.; Yang, Y.; Qiu, Z.; Che, Z.; Du, T. Integrated optimization for utilizing iron and steel industry's waste heat with urban heating based on exergy analysis. *Energy Convers. Manag.* **2023**, *295*, 117593. [CrossRef]
64. Gan, L.; Yang, T.; Wang, B.; Chen, X.; Hua, H.; Dong, Z.Y. Three-stage coordinated operation of steel plant-based multi-energy microgrids considering carbon reduction. *Energy* **2023**, *278*, 127639. [CrossRef]
65. Zhang, C.; Xu, Y.; Dong, Z.Y.; Yang, L.F. Multitime scale coordinated adaptive robust operation for industrial multienergy microgrids with load allocation. *IEEE Trans. Ind. Inform.* **2020**, *16*, 3051–3063. [CrossRef]
66. Power Demand-Side Flexibility 2025. Rocky Mountain Institute (RMI). Available online: https://rmi.org.cn/insights/industrial-dsf/ (accessed on 25 December 2023). (In Chinese).
67. Pena, J.G.C.; de Oliveira, V.B.; Salles, J.L.F. Optimal scheduling of a by-product gas supply system in the iron- and steel-making process under uncertainties. *Comput. Chem. Eng.* **2019**, *125*, 351–364. [CrossRef]
68. Zhao, X.C.; Bai, H.; Shi, Q.; Lu, X.; Zhang, Z.H. Optimal scheduling of a byproduct gas system in a steel plant considering time-of-use electricity pricing. *Appl. Energy* **2017**, *195*, 100–113. [CrossRef]
69. Yang, J.; Cai, J.; Sun, W.; Huang, J. Optimal allocation of surplus gas and suitable capacity for buffer users in steel plant. *Appl. Therm. Eng.* **2017**, *115*, 586–596. [CrossRef]
70. Duan, W.; Li, R.; Yang, S.; Han, J.; Lv, X.; Wang, Z.; Yu, Q. Theoretical study on coal gasification behavior in CO_2 atmosphere driven by slag waste heat. *Energy* **2024**, *305*, 132269. [CrossRef]

71. Ja'Fari, M.; Khan, M.I.; Al-Ghamdi, S.G.; Jaworski, A.J.; Asfand, F. Waste heat recovery in iron and steel industry using organic Rankine cycles. *Chem. Eng. J.* **2023**, *477*, 146925. [CrossRef]
72. Ding, X.; Xu, J.; Sun, Y.; Liao, S.; Zheng, J. A demand side controller of electrolytic aluminum industrial microgrids considering wind power fluctuations. *Prot. Control Mod. Power Syst.* **2022**, *7*, 1–13. [CrossRef]
73. Yu, Q.; Xu, J.; Liao, S.; Liu, H. Adaptive load control of electrolytic aluminum for power system frequency regulation based on the aluminum production operation state. *Energy Rep.* **2022**, *8*, 1259–1269. [CrossRef]
74. Sgouridis, S.; Ali, M.; Sleptchenko, A.; Bouabid, A.; Ospina, G. Aluminum smelters in the energy transition: Optimal configuration and operation for renewable energy integration in high insolation regions. *Renew. Energy* **2021**, *180*, 937–953. [CrossRef]
75. Wazirali, R.; Yaghoubi, E.; Abujazar, M.S.S.; Ahmad, R.; Vakili, A.H. State-of-the-art review on energy and load forecasting in microgrids using artificial neural networks, machine learning, and deep learning techniques. *Electr. Power Syst. Res.* **2023**, *225*, 109792. [CrossRef]
76. Yao, H.; Qu, P.; Qin, H.; Lou, Z.; Wei, X.; Song, H. Multidimensional electric power parameter time series forecasting and anomaly fluctuation analysis based on the AFFC-GLDA-RL method. *Energy* **2024**, *313*, 134180. [CrossRef]
77. Benti, N.E.; Chaka, M.D.; Semie, A.G. Forecasting renewable energy generation with machine learning and deep learning: Current advances and future prospects. *Sustainability* **2023**, *15*, 7087. [CrossRef]
78. Judge, M.A.; Franzitta, V.; Curto, D.; Guercio, A.; Cirrincione, G.; Khattak, H.A. A comprehensive review of artificial intelligence approaches for smart grid integration and optimization. *Energy Convers. Manag. X* **2024**, *24*, 100724. [CrossRef]
79. Kuster, C.; Rezgui, Y.; Mourshed, M. Electrical load forecasting models: A critical systematic review. *Sustain. Cities Soc.* **2017**, *35*, 257–270. [CrossRef]
80. Maharana, K.; Mondal, S.; Nemade, B. A review: Data pre-processing and data augmentation techniques. *Glob. Transit. Proc.* **2022**, *3*, 91–99. [CrossRef]
81. Liu, H.; Chen, C. Data processing strategies in wind energy forecasting models and applications: A comprehensive review. *Appl. Energy* **2019**, *249*, 392–408. [CrossRef]
82. Fan, C.; Chen, M.; Wang, X.; Wang, J.; Huang, B. A review on data preprocessing techniques toward efficient and reliable knowledge discovery from building operational data. *Front. Energy Res.* **2021**, *9*, 652801. [CrossRef]
83. Hosseinzadeh, M.; Azhir, E.; Ahmed, O.H.; Ghafour, M.Y.; Ahmed, S.H.; Rahmani, A.M.; Vo, B. Data cleansing mechanisms and approaches for big data analytics: A systematic study. *J. Ambient. Intell. Humaniz. Comput.* **2023**, *14*, 99–111. [CrossRef]
84. Altowaijri, S.M. Efficient data aggregation and duplicate removal using grid-based hashing in cloud-assisted industrial IoT. *IEEE Access* **2024**, *12*, 145350–145365. [CrossRef]
85. Jurj, D.I.; Czumbil, L.; Bârgăuan, B.; Ceclan, A.; Polycarpou, A.; Micu, D.D. Custom outlier detection for electrical energy consumption data applied in case of demand response in block of buildings. *Sensors* **2021**, *21*, 2946. [CrossRef]
86. Ariyaluran Habeeb, R.A.; Nasaruddin, F.; Gani, A.; Targio Hashem, I.A.; Ahmed, E.; Imran, M. Real-time big data processing for anomaly detection: A Survey. *Int. J. Inf. Manag.* **2019**, *45*, 289–307. [CrossRef]
87. Himeur, Y.; Ghanem, K.; Alsalemi, A.; Bensaali, F.; Amira, A. Artificial intelligence based anomaly detection of energy consumption in buildings: A review, current trends and new perspectives. *Appl. Energy* **2021**, *287*, 116601. [CrossRef]
88. Chen, Z.; Zhang, B.; Du, C.; Yang, C.; Gui, W. Outlier-adaptive-based non-crossing quantiles method for day-ahead electricity price forecasting. *Appl. Energy* **2025**, *382*, 125328. [CrossRef]
89. Liang, Y. Outlier detection model of electric power big data based on fuzzy K-means clustering algorithm. In Proceedings of the 2023 International Conference on Networking, Informatics and Computing (ICNETIC), Palermo, Italy, 29–31 May 2023; pp. 703–707. [CrossRef]
90. Oza, P.; Patel, V.M. One-class convolutional neural network. *IEEE Signal Process. Lett.* **2019**, *26*, 277–281. [CrossRef]
91. Zhang, L.; Wan, L.; Xiao, Y.; Li, S.; Zhu, C. Anomaly detection method of smart meters data based on GMM-LDA clustering feature learning and PSO support vector machine. In Proceedings of the 2019 IEEE Sustainable Power and Energy Conference (iSPEC), Beijing, China, 21–23 November 2019; pp. 2407–2412. [CrossRef]
92. Yozgatligil, C.; Aslan, S.; Iyigun, C.; Batmaz, I. Comparison of missing value imputation methods in time series: The case of Turkish meteorological data. *Theor. Appl. Climatol.* **2013**, *112*, 143–167. [CrossRef]
93. Lin, W.C.; Tsai, C.F. Missing value imputation: A review and analysis of the literature (2006–2017). *Artif. Intell. Rev.* **2020**, *53*, 1487–1509. [CrossRef]
94. Faisal, S.; Tutz, G. Multiple imputation using nearest neighbor methods. *Inf. Sci.* **2021**, *570*, 500–516. [CrossRef]
95. Ren, L.; Wang, T.; Sekhari Seklouli, A.; Zhang, H.; Bouras, A. A review on missing values for main challenges and methods. *Inf. Syst.* **2023**, *119*, 102268. [CrossRef]
96. Wang, M.C.; Tsai, C.F.; Lin, W.C. Towards missing electric power data imputation for energy management systems. *Expert Syst. Appl.* **2021**, *174*, 114743. [CrossRef]
97. Lotfipoor, A.; Patidar, S.; Jenkins, D.P. Transformer network for data imputation in electricity demand data. *Energy Build.* **2023**, *300*, 113675. [CrossRef]

98. Bülte, C.; Kleinebrahm, M.; Yilmaz, H.Ü.; Gómez-Romero, J. Multivariate time series imputation for energy data using neural networks. *Energy AI* **2023**, *13*, 100239. [CrossRef]
99. Jeong, D.; Park, C.; Ko, Y.M. Missing data imputation using mixture factor analysis for building electric load data. *Appl. Energy* **2021**, *304*, 117655. [CrossRef]
100. Ruggles, T.H.; Farnham, D.J.; Tong, D.; Caldeira, K. Developing reliable hourly electricity demand data through screening and imputation. *Sci. Data* **2020**, *7*, 155. [CrossRef] [PubMed]
101. Fernandes, V.; Carvalho, G.; Pereira, V.; Bernardino, J. Analyzing data reduction techniques: An experimental perspective. *Appl. Sci.* **2024**, *14*, 3436. [CrossRef]
102. Zhu, J.; Dong, H.; Zheng, W.; Li, S.; Huang, Y.; Xi, L. Review and prospect of data-driven techniques for load forecasting in integrated energy systems. *Appl. Energy* **2022**, *321*, 119269. [CrossRef]
103. Khoei, T.T.; Singh, A. Data reduction in big data: A survey of methods, challenges and future directions. *Int. J. Data Sci. Anal.* **2024**, 1–40. [CrossRef]
104. Habib, M.D.A.; Hossain, M.J. Advanced feature engineering in microgrid PV forecasting: A fast computing and data-driven hybrid modeling framework. *Renew. Energy* **2024**, *235*, 121258. [CrossRef]
105. Jia, W.; Sun, M.; Lian, J.; Hou, S. Feature dimensionality reduction: A review. *Complex. Intell. Syst.* **2022**, *8*, 2663–2693. [CrossRef]
106. Khaire, U.M.; Dhanalakshmi, R. Stability of feature selection algorithm: A review. *J. King Saud. Univ.—Comput. Inf. Sci.* **2022**, *34*, 1060–1073. [CrossRef]
107. Cherrington, M.; Thabtah, F.; Lu, J.; Xu, Q. Feature selection: Filter methods performance challenges. In Proceedings of the 2019 International Conference on Computer and Information Sciences (ICCIS), Sakaka, Saudi Arabia, 3–4 April 2019; pp. 1–4. [CrossRef]
108. Suntrakumar, M.V.; Binti Syed Ahmad, S.S.; Samsudin, M.L.; Othman, M.R. Comparative analysis of filter, wrapper, and embedded feature selection methods to predict load progression in combined cycle power plant (CCPP) startup across diverse startup classes. In Proceedings of the 2024 8th International Conference on Power Energy Systems and Applications (ICoPESA), Hong Kong, China, 24–26 June 2024; pp. 127–135. [CrossRef]
109. Liu, L.; Fu, Q.; Lu, Y.; Wang, Y.; Wu, H.; Chen, J. CorrDQN-FS: A two-stage feature selection method for energy consumption prediction via deep reinforcement learning. *J. Build. Eng.* **2023**, *80*, 108044. [CrossRef]
110. Salcedo-Sanz, S.; Cornejo-Bueno, L.; Prieto, L.; Paredes, D.; García-Herrera, R. Feature selection in machine learning prediction systems for renewable energy applications. *Renew. Sustain. Energy Rev.* **2018**, *90*, 728–741. [CrossRef]
111. Amer, H.N.; Dahlan, N.Y.; Azmi, A.M.; Latip, M.F.A.; Onn, M.S.; Tumian, A. Solar power prediction based on artificial neural network guided by feature selection for large-scale solar photovoltaic plant. *Energy Rep.* **2023**, *9*, 262–266. [CrossRef]
112. Jahani, A.; Zare, K.; Mohammad Khanli, L. Short-term load forecasting for microgrid energy management system using hybrid SPM-LSTM. *Sustain. Cities Soc.* **2023**, *98*, 104775. [CrossRef]
113. Alcañiz, A.; Grzebyk, D.; Ziar, H.; Isabella, O. Trends and gaps in photovoltaic power forecasting with machine learning. *Energy Rep.* **2023**, *9*, 447–471. [CrossRef]
114. Zhang, Y.; Jia, M.; Wen, H.; Bian, Y.; Shi, Y. Toward value-oriented renewable energy forecasting: An iterative learning approach. *IEEE Trans. Smart Grid* **2025**, *16*, 1962–1974. [CrossRef]
115. Iheanetu, K.J. Solar Photovoltaic power forecasting: A review. *Sustainability* **2022**, *14*, 17005. [CrossRef]
116. Ahmed, A.; Khalid, M. A review on the selected applications of forecasting models in renewable power systems. *Renew. Sustain. Energy Rev.* **2019**, *100*, 9–21. [CrossRef]
117. Niu, D.; Sun, L.; Yu, M.; Wang, K. Point and interval forecasting of ultra-short-term wind power based on a data-driven method and hybrid deep learning model. *Energy* **2022**, *254*, 124384. [CrossRef]
118. Zhang, Y.; Pan, G.; Zhao, Y.; Li, Q.; Wang, F. Short-term wind speed interval prediction based on artificial intelligence methods and error probability distribution. *Energy Convers. Manag.* **2020**, *224*, 113346. [CrossRef]
119. Chang, Q.; Wang, Y.; Lu, X.; Shi, D.; Li, H.; Duan, J.; Wang, Z. Probabilistic load forecasting via point forecast feature integration. In Proceedings of the 2019 IEEE Innovative Smart Grid Technologies—Asia (ISGT Asia), Chengdu, China, 21–24 May 2019; pp. 99–104. [CrossRef]
120. Aguilar, D.; Quinones, J.J.; Pineda, L.R.; Ostanek, J.; Castillo, L. Optimal scheduling of renewable energy microgrids: A robust multi-objective approach with machine learning-based probabilistic forecasting. *Appl. Energy* **2024**, *369*, 123548. [CrossRef]
121. Nian, R.; Liu, J.; Huang, B. A review on reinforcement learning: Introduction and applications in industrial process control. *Comput. Chem. Eng.* **2020**, *139*, 106886. [CrossRef]
122. Talaei Khoei, T.; Ould Slimane, H.; Kaabouch, N. Deep learning: Systematic review, models, challenges, and research directions. *Neural Comput. Applic* **2023**, *35*, 23103–23124. [CrossRef]
123. Mienye, I.D.; Swart, T.G. A comprehensive review of deep learning: Architectures, recent advances, and applications. *Information* **2024**, *15*, 755. [CrossRef]

124. Yaghoubi, E.; Yaghoubi, E.; Khamees, A.; Razmi, D.; Lu, T. A systematic review and meta-analysis of machine learning, deep learning, and ensemble learning approaches in predicting EV charging behavior. *Eng. Appl. Artif. Intell.* **2024**, *135*, 108789. [CrossRef]
125. Voyant, C.; Notton, G.; Kalogirou, S.; Nivet, M.-L.; Paoli, C.; Motte, F.; Fouilloy, A. Machine learning methods for solar radiation forecasting: A review. *Renew. Energy* **2017**, *105*, 569–582. [CrossRef]
126. Saidi, A.; Ben Othman, S.; Dhouibi, M.; Ben Saoud, S. FPGA-based implementation of classification techniques: A survey. *Integration* **2021**, *81*, 280–299. [CrossRef]
127. Zendehboudi, A.; Baseer, M.A.; Saidur, R. Application of support vector machine models for forecasting solar and wind energy resources: A review. *J. Clean. Prod.* **2018**, *199*, 272–285. [CrossRef]
128. Krzywinski, M.; Altman, N. Classification and regression trees. *Nat. Methods* **2017**, *14*, 757–758. [CrossRef]
129. Liu, D.; Sun, K. Random forest solar power forecast based on classification optimization. *Energy* **2019**, *187*, 115940. [CrossRef]
130. Yang, X.; Fu, G.; Zhang, Y.; Kang, N.; Gao, F. A Naive Bayesian wind power interval prediction approach based on rough set attribute reduction and weight optimization. *Energies* **2017**, *10*, 1903. [CrossRef]
131. Wickramasinghe, I.; Kalutarage, H. Naive Bayes: Applications, variations and vulnerabilities: A review of literature with code snippets for implementation. *Soft Comput.* **2021**, *25*, 2277–2293. [CrossRef]
132. Dong, Y.; Ma, X.; Fu, T. Electrical load forecasting: A deep learning approach based on *K*-nearest neighbors. *Appl. Soft Comput.* **2021**, *99*, 106900. [CrossRef]
133. Yildiz, B.; Bilbao, J.I.; Sproul, A.B. A review and analysis of regression and machine learning models on commercial building electricity load forecasting. *Renew. Sustain. Energy Rev.* **2017**, *73*, 1104–1122. [CrossRef]
134. Abdullah, B.U.D.; Khanday, S.A.; Islam, N.U.; Lata, S.; Fatima, H.; Nengroo, S.H. Comparative analysis using multiple regression models for forecasting photovoltaic power generation. *Energies* **2024**, *17*, 1564. [CrossRef]
135. Belany, P.; Hrabovsky, P.; Sedivy, S.; Cajova Kantova, N.; Florkova, Z. A comparative analysis of polynomial regression and artificial neural networks for prediction of lighting consumption. *Buildings* **2024**, *14*, 1712. [CrossRef]
136. Li, Y.; Yang, R.; Wang, X.; Zhu, J.; Song, N. Carbon price combination forecasting model based on lasso regression and optimal integration. *Sustainability* **2023**, *15*, 9354. [CrossRef]
137. Saini, V.K.; Kumar, R.; Al-Sumaiti, A.S.; Sujil, A.; Heydarian-Forushani, E. Learning based short term wind speed forecasting models for smart grid applications: An extensive review and case study. *Electr. Power Syst. Res.* **2023**, *222*, 109502. [CrossRef]
138. Awad, M.; Khanna, R. Support Vector Regression. In *Efficient Learning Machines: Theories, Concepts, and Applications for Engineers and System Designers*; Apress: Berkeley, CA, USA, 2015; pp. 67–80. [CrossRef]
139. Singh Kushwah, J.; Kumar, A.; Patel, S.; Soni, R.; Gawande, A.; Gupta, S. Comparative study of regressor and classifier with decision tree using modern tools. *Mater. Today: Proc.* **2022**, *56*, 3571–3576. [CrossRef]
140. Markovics, D.; Mayer, M.J. Comparison of machine learning methods for photovoltaic power forecasting based on numerical weather prediction. *Renew. Sustain. Energy Rev.* **2022**, *161*, 112364. [CrossRef]
141. Gaboitaolelwe, J.; Zungeru, A.M.; Yahya, A.; Lebekwe, C.K.; Vinod, D.N.; Salau, A.O. Machine learning based solar photovoltaic power forecasting: A review and comparison. *IEEE Access* **2023**, *11*, 40820–40845. [CrossRef]
142. Habbak, H.; Mahmoud, M.; Metwally, K.; Fouda, M.M.; Ibrahem, M.I. Load forecasting techniques and their applications in smart grids. *Energies* **2023**, *16*, 1480. [CrossRef]
143. Ikotun, A.M.; Ezugwu, A.E.; Abualigah, L.; Abuhaija, B.; Heming, J. K-means clustering algorithms: A comprehensive review, variants analysis, and advances in the era of big data. *Inf. Sci.* **2023**, *622*, 178–210. [CrossRef]
144. Saxena, A.; Prasad, M.; Gupta, A.; Bharill, N.; Patel, O.P.; Tiwari, A.; Er, M.J.; Ding, W.; Lin, C.-T. A review of clustering techniques and developments. *Neurocomputing* **2017**, *267*, 664–681. [CrossRef]
145. Zhang, C.; Li, R. A novel closed-loop clustering algorithm for hierarchical load forecasting. *IEEE Trans. Smart Grid* **2021**, *12*, 432–441. [CrossRef]
146. Ran, X.; Xi, Y.; Lu, Y.; Wang, X.; Lu, Z. Comprehensive survey on hierarchical clustering algorithms and the recent developments. *Artif. Intell. Rev.* **2023**, *56*, 8219–8264. [CrossRef]
147. Wang, H.; Zhang, J.; Shen, Y.; Wang, S.; Deng, B.; Zhao, W. Improved density peak clustering with a flexible manifold distance and natural nearest neighbors for network intrusion detection. *Sci. Rep.* **2025**, *15*, 8510. [CrossRef]
148. Greenacre, M.; Groenen, P.J.F.; Hastie, T.; D'Enza, A.I.; Markos, A.; Tuzhilina, E. Principal component analysis. *Nat. Rev. Methods Primers* **2022**, *2*, 1–21. [CrossRef]
149. Li, Y.; Zhang, M.; Bian, X.; Tian, L.; Tang, C. Progress of independent component analysis and its recent application in spectroscopy quantitative analysis. *Microchem. J.* **2024**, *202*, 110836. [CrossRef]
150. Huang, J.; Wang, F.; Qiao, L.; Yang, X. T-distributed stochastic neighbor embedding echo state network with state matrix dimensionality reduction for time series prediction. *Eng. Appl. Artif. Intell.* **2023**, *122*, 106055. [CrossRef]
151. Canese, L.; Cardarilli, G.C.; Di Nunzio, L.; Fazzolari, R.; Giardino, D.; Re, M.; Spanò, S. Multi-agent reinforcement learning: A review of challenges and applications. *Appl. Sci.* **2021**, *11*, 4948. [CrossRef]

152. Upadhyaya, A.; Rahul. Optimizing plant health with Q-Learning: A deep reinforcement learning approach. In Proceedings of the 2024 15th International Conference on Computing Communication and Networking Technologies (ICCCNT), Mandi, India, 24–28 June 2024; pp. 1–5. [CrossRef]
153. LeCun, Y.; Bengio, Y.; Hinton, G. Deep learning. *Nature* **2015**, *521*, 436–444. [CrossRef] [PubMed]
154. Zhang, L.; Wen, J.; Li, Y.; Chen, J.; Ye, Y.; Fu, Y.; Livingood, W. A review of machine learning in building load prediction. *Appl. Energy* **2021**, *285*, 116452. [CrossRef]
155. Mosavi, A.; Salimi, M.; Faizollahzadeh Ardabili, S.; Rabczuk, T.; Shamshirband, S.; Varkonyi-Koczy, A.R. State of the art of machine learning models in energy systems, a systematic review. *Energies* **2019**, *12*, 1301. [CrossRef]
156. Messaoud, S.; Bradai, A.; Bukhari, S.H.R.; Quang, P.T.A.; Ahmed, O.B.; Atri, M. A survey on machine learning in Internet of Things: Algorithms, strategies, and applications. *Internet Things* **2020**, *12*, 100314. [CrossRef]
157. Song, X.; Deng, L.; Wang, H.; Zhang, Y.; He, Y.; Cao, W. Deep learning-based time series forecasting. *Artif. Intell. Rev.* **2024**, *58*, 23. [CrossRef]
158. Gu, J.; Wang, Z.; Kuen, J.; Ma, L.; Shahroudy, A.; Shuai, B.; Liu, T.; Wang, X.; Wang, G.; Cai, J.; et al. Recent advances in convolutional neural networks. *Pattern Recognit.* **2018**, *77*, 354–377. [CrossRef]
159. Liu, X.; Wang, W. Deep time series forecasting models: A comprehensive survey. *Mathematics* **2024**, *12*, 1504. [CrossRef]
160. Mienye, I.D.; Swart, T.G.; Obaido, G. Recurrent neural networks: A comprehensive review of architectures, variants, and applications. *Information* **2024**, *15*, 517. [CrossRef]
161. Lee, C. A review of data analytics in technological forecasting. *Forecast. Soc. Change* **2021**, *166*, 120646. [CrossRef]
162. Rainio, O.; Teuho, J.; Klén, R. Evaluation metrics and statistical tests for machine learning. *Sci. Rep.* **2024**, *14*, 6086. [CrossRef]
163. Antonanzas, J.; Osorio, N.; Escobar, R.; Urraca, R.; Martinez-de-Pison, F.J.; Antonanzas-Torres, F. Review of photovoltaic power forecasting. *Sol. Energy* **2016**, *136*, 78–111. [CrossRef]
164. Zhou, D.X.; Liu, Y.J.; Wang, X.; Wang, F.X.; Jia, Y. Research progress of photovoltaic power prediction technology based on artificial intelligence methods. *Energy Eng.* **2024**, *121*, 3573–3616. [CrossRef]
165. Hou, H.; Liu, C.; Wang, Q.; Wu, X.; Tang, J.; Shi, Y.; Xie, C. Review of load forecasting based on artificial intelligence methodologies, models, and challenges. *Electr. Power Syst. Res.* **2022**, *210*, 108067. [CrossRef]
166. Barak, S.; Mokfi, T. Evaluation and selection of clustering methods using a hybrid group MCDM. *Expert Syst. Appl.* **2019**, *138*, 112817. [CrossRef]
167. Sen, S.; Kumar, V. Microgrid modelling: A comprehensive survey. *Annu. Rev. Control* **2018**, *46*, 216–250. [CrossRef]
168. Alzahrani, A.; Ferdowsi, M.; Shamsi, P.; Dagli, C.H. Modeling and simulation of microgrid. *Procedia Comput. Sci.* **2017**, *114*, 392–400. [CrossRef]
169. Liu, R.; Liu, X.; Tang, J.; Han, H.; Su, M.; Huang, Y. Multi-timescale dispatching method for industrial microgrid considering electrolytic aluminum load characteristics. *Processes* **2025**, *13*, 1411. [CrossRef]
170. Liu, Z.Y.; Shao, B.; Zhang, Y.J.; Liu, D.; Kong, Z.W.; Nai, J.H. Load modeling and analysis considering the impact of microgrid integration. In Proceedings of the 2024 21st International Conference on Harmonics and Quality of Power (ICHQP), Chengdu, China, 15–18 October 2024; pp. 215–219. [CrossRef]
171. Amarendra Reddy, B.; Bhukya, C.N.; Venkatesh, A. Constant power load in DC microgrid system: A passivity based control of two input integrated DC-DC converter. *E-Prime—Adv. Electr. Eng. Electron. Energy* **2025**, *11*, 100941. [CrossRef]
172. Chávarro-Barrera, L.; Pérez-Londoño, S.; Mora-Flórez, J. An adaptive approach for Dynamic Load Modeling in Microgrids. *IEEE Trans. Smart Grid* **2021**, *12*, 2834–2843. [CrossRef]
173. Wang, W.; Wang, D.; Zhao, Y.; Yu, Y.; Wang, Y. Research on capacity optimization and real-time control of island microgrid considering time-shifting load. *Energy Rep.* **2022**, *8*, 990–997. [CrossRef]
174. Zhang, Z.; Wang, P.; Zhou, J.; Wang, W.; Xu, D. A novel passivity model predictive control for predefined-time feedforward compensation in DC microgrids feeding constant power Loads. *IEEE Trans. Power Electron.* **2025**, *40*, 5147–5162. [CrossRef]
175. Xia, S.; Luo, X.; Chan, K.W.; Zhou, M.; Li, G. Probabilistic transient stability constrained optimal power flow for power systems with multiple correlated uncertain wind generations. *IEEE Trans. Sustain. Energy* **2016**, *7*, 1133–1144. [CrossRef]
176. Li, Y.; Li, K.; Yang, Z.; Yu, Y.; Xu, R.; Yang, M. Stochastic optimal scheduling of demand response-enabled microgrids with renewable generations: An analytical-heuristic approach. *J. Clean. Prod.* **2022**, *330*, 129840. [CrossRef]
177. Li, Y.; Yang, Z.; Li, G.; Mu, Y.; Zhao, D.; Chen, C.; Shen, B. Optimal scheduling of isolated microgrid with an electric vehicle battery swapping station in multi-stakeholder scenarios: A bi-level programming approach via real-time pricing. *Appl. Energy* **2018**, *232*, 54–68. [CrossRef]
178. Wang, L.; Lin, J.; Dong, H.; Wang, Y.; Zeng, M. Demand response comprehensive incentive mechanism-based multi-time scale optimization scheduling for park integrated energy system. *Energy* **2023**, *270*, 126893. [CrossRef]
179. Huang, S.; Abedinia, O. Investigation in economic analysis of microgrids based on renewable energy uncertainty and demand response in the electricity market. *Energy* **2021**, *225*, 120247. [CrossRef]

180. Pan, C.; Jin, T.; Li, N.; Wang, G.; Hou, X.; Gu, Y. Multi-objective and two-stage optimization study of integrated energy systems considering P2G and integrated demand responses. *Energy* **2023**, *270*, 126846. [CrossRef]
181. Xu, C.; Wu, X.; Shan, Z.; Zhang, Q.; Dang, B.; Wang, Y.; Wang, F.; Jiang, X.; Xue, Y.; Shi, C. Bi-level configuration and operation collaborative optimization of shared hydrogen energy storage system for a wind farm cluster. *J. Energy Storage* **2024**, *86*, 111107. [CrossRef]
182. Guan, Z.; Wang, H.; Li, Z.; Luo, X.; Yang, X.; Fang, J.; Zhao, Q. Multi-objective optimal scheduling of microgrids based on improved particle swarm algorithm. *Energies* **2024**, *17*, 1760. [CrossRef]
183. Banihabib, R.; Fadnes, F.S.; Assadi, M. Techno-economic optimization of microgrid operation with integration of renewable energy, hydrogen storage, and micro gas turbine. *Renew. Energy* **2024**, *237*, 121708. [CrossRef]
184. Kang, J.-N.; Liu, L.; Liu, L.; Wei, Y.-M. Operation strategy for a net-zero emissions park microgrid with multi-stakeholders: A multi-objective with bi-level optimization approach. *Energy* **2025**, *321*, 135524. [CrossRef]
185. Zhang, Y.; Ren, Y.; Liu, Z.; Li, H.; Jiang, H.; Xue, Y.; Ou, J.; Hu, R.; Zhang, J.; Gao, D.W. Federated deep reinforcement learning for varying-scale multi-energy microgrids energy management considering comprehensive security. *Appl. Energy* **2025**, *380*, 125072. [CrossRef]
186. Zheng, Y.; Wang, H.; Wang, J.; Wang, Z.; Zhao, Y. Optimal scheduling strategy of electricity and thermal energy storage based on soft actor-critic reinforcement learning approach. *J. Energy Storage* **2024**, *92*, 112084. [CrossRef]
187. Huang, W.; Zhang, B.; Ge, L.; He, J.; Liao, W.; Ma, P. Day-ahead optimal scheduling strategy for electrolytic water to hydrogen production in zero-carbon parks type microgrid for optimal utilization of electrolyzer. *J. Energy Storage* **2023**, *68*, 107653. [CrossRef]
188. Shen, X.; Zhang, X.; Li, G.; Lie, T.T.; Hong, L. Experimental study on the external electrical thermal and dynamic power characteristics of alkaline water electrolyzer. *Int. J. Energy Res.* **2018**, *42*, 3244–3257. [CrossRef]
189. Darmawan, A.; Fauziah, K.; Zaky, T.; Astriani, Y.; Kurniasari, A.; Kurniawan; Hapsari, A.U.; Pravitasari, R.D.; Agustanhakri; Rahayu, S.; et al. Integrating fuel cell technology in microgrid systems for lower carbon emission. In *Decarbonizing Power Generation Sectors Using Biomass and Hydrogen-Based Fuels: A Roadmap to Sustainable Energy Transformation*; Springer Nature: Singapore, 2025; pp. 239–278. [CrossRef]
190. Eichhorn Colombo, K.W.; Kharton, V.V.; Berto, F.; Paltrinieri, N. Mathematical modeling and simulation of hydrogen-fueled solid oxide fuel cell system for micro-grid applications—Effect of failure and degradation on transient performance. *Energy* **2020**, *202*, 117752. [CrossRef]
191. Swain, R.; Behera, P.K.; Sarkar, I.; Pattnaik, M. Optimizing reliability of PV-based microgrid by integrating fuel cell. In *Emerging Electronics and Automation*; Springer Nature: Singapore, 2025; pp. 73–84. [CrossRef]
192. Mei, Y.; Li, B.; Wang, H.; Wang, X.; Negnevitsky, M. Multi-objective optimal scheduling of microgrid with electric vehicles. *Energy Rep.* **2022**, *8*, 4512–4524. [CrossRef]
193. Güven, A.F. Integrating electric vehicles into hybrid microgrids: A stochastic approach to future-ready renewable energy solutions and management. *Energy* **2024**, *303*, 131968. [CrossRef]
194. Li, Y.; Wang, C.; Li, G.; Chen, C. Optimal scheduling of integrated demand response-enabled integrated energy systems with uncertain renewable generations: A Stackelberg game approach. *Energy Convers. Manag.* **2021**, *235*, 113996. [CrossRef]
195. Sharma, B.; Gupta, N.; Niazi, K.R.; Swarnkar, A. Estimating impact of price-based demand response in contemporary distribution systems. *Int. J. Electr. Power Energy Syst.* **2022**, *135*, 107549. [CrossRef]
196. Yang, Y.; Wang, J.; Zhao, P.; Dong, Y.; Fan, X. Collaborative planning and optimal scheduling for a specific distribution network area containing multiple microgrids based on a Game-theoretic approach. *Sustain. Energy Grids Netw.* **2025**, *41*, 101625. [CrossRef]
197. Li, Y.; Su, Y.; Zhang, Y.; Wu, W.; Xia, L. Two-layered optimal scheduling under a semi-model architecture of hydro-wind-solar multi-energy systems with hydrogen storage. *Energy* **2024**, *313*, 134115. [CrossRef]
198. Wu, N.; Wang, Z.; Li, X.; Lei, L.; Qiao, Y.; Linghu, J.; Huang, J. Research on real-time coordinated optimization scheduling control strategy with supply-side flexibility in multi-microgrid energy systems. *Renew. Energy* **2025**, *238*, 121976. [CrossRef]
199. Zhang, W.; Xu, Y. Distributed optimal control for multiple microgrids in a distribution network. *IEEE Trans. Smart Grid* **2019**, *10*, 3765–3779. [CrossRef]
200. Moretti, L.; Meraldi, L.; Niccolai, A.; Manzolini, G.; Leva, S. An innovative tunable rule-based strategy for the predictive management of hybrid microgrids. *Electronics* **2021**, *10*, 1162. [CrossRef]
201. Zhu, B.; Wang, D. Master-slave game optimal scheduling for multi-agent integrated energy system based on uncertainty and demand response. *Sustainability* **2024**, *16*, 3182. [CrossRef]
202. Coelho, F.C.; Assis, F.A.; Castro, J.F.C.; Donadon, A.R.; Roncolatto, R.A.; Andrade, V.E.; Rosas, P.A.; Barcelos, S.L.; Saavedra, O.R.; Bento, R.G.; et al. Monte Carlo simulation of community microgrid operation: Business prospects in the Brazilian regulatory framework. *Util. Policy* **2025**, *92*, 101856. [CrossRef]
203. Thirunavukkarasu, G.S.; Seyedmahmoudian, M.; Jamei, E.; Horan, B.; Mekhilef, S.; Stojcevski, A. Role of optimization techniques in microgrid energy management systems-A review. *Energy Strategy Rev.* **2022**, *43*, 100899. [CrossRef]

204. Bakhtiari, H.; Zhong, J.; Alvarez, M. Predicting the stochastic behavior of uncertainty sources in planning a stand-alone renewable energy-based microgrid using Metropolis-coupled Markov chain Monte Carlo simulation. *Appl. Energy* **2021**, *290*, 116719. [CrossRef]
205. Boroumandfar, G.; Khajehzadeh, A.; Eslami, M. A single and multiobjective robust optimization of a microgrid in distribution network considering uncertainty risk. *Sci. Rep.* **2024**, *14*, 28195. [CrossRef]
206. He, Y.; Li, Z.; Zhang, J.; Shi, G.; Cao, W. Day-ahead and intraday multi-time scale microgrid scheduling based on light robustness and MPC. *Int. J. Electr. Power Energy Syst.* **2023**, *144*, 108546. [CrossRef]
207. Budiman, F.N.; Ramli, M.A.; Milyani, A.H.; Bouchekara, H.R.; Rawa, M.; Muktiadji, R.F.; Seedahmed, M.M. Stochastic optimization for the scheduling of a grid-connected microgrid with a hybrid energy storage system considering multiple uncertainties. *Energy Rep.* **2022**, *8*, 7444–7456. [CrossRef]
208. Abunima, H.; Park, W.-H.; Glick, M.B.; Kim, Y.-S. Two-Stage stochastic optimization for operating a Renewable-Based Microgrid. *Appl. Energy* **2022**, *325*, 119848. [CrossRef]
209. Yang, M.; Wang, J.; Chen, Y.; Zeng, Y.; Su, X. Data-driven robust optimization scheduling for microgrid day-ahead to intra-day operations based on renewable energy interval prediction. *Energy* **2024**, *313*, 134058. [CrossRef]
210. Yang, J.; Su, C. Robust optimization of microgrid based on renewable distributed power generation and load demand uncertainty. *Energy* **2021**, *223*, 120043. [CrossRef]
211. Li, Y.; Zhang, F.; Li, Y.; Wang, Y. An improved two-stage robust optimization model for CCHP-P2G microgrid system considering multi-energy operation under wind power outputs uncertainties. *Energy* **2021**, *223*, 120048. [CrossRef]
212. Li, S.; Zhu, J.; Dong, H.; Zhu, H.; Fan, J. A novel rolling optimization strategy considering grid-connected power fluctuations smoothing for renewable energy microgrids. *Appl. Energy* **2022**, *309*, 118441. [CrossRef]
213. Shen, W.J.; Zeng, B.; Zeng, M. Multi-timescale rolling optimization dispatch method for integrated energy system with hybrid energy storage system. *Energy* **2023**, *283*, 129006. [CrossRef]
214. Zhang, G.; Li, Y.; Xie, T.; Zhang, K. Two-stage rolling optimization operation strategy for microgrid considering BESU state. *Int. J. Electr. Power Energy Syst.* **2025**, *165*, 110497. [CrossRef]
215. Yang, X.; Wang, X.; Leng, Z.; Deng, Y.; Deng, F.; Zhang, Z.; Yang, L.; Liu, X. An optimized scheduling strategy combining robust optimization and rolling optimization to solve the uncertainty of RES-CCHP MG. *Renew. Energy* **2023**, *211*, 307–325. [CrossRef]
216. Basir Khan, M.R.; Jidin, R.; Pasupuleti, J. Multi-agent based distributed control architecture for microgrid energy management and optimization. *Energy Convers. Manag.* **2016**, *112*, 288–307. [CrossRef]
217. Javanmard, B.; Tabrizian, M.; Ansarian, M.; Ahmarinejad, A. Energy management of multi-microgrids based on game theory approach in the presence of demand response programs, energy storage systems and renewable energy resources. *J. Energy Storage* **2021**, *42*, 102971. [CrossRef]
218. Wang, C.; Wang, M.; Wang, A.; Zhang, X.; Zhang, J.; Ma, H.; Yang, N.; Zhao, Z.; Lai, C.S.; Lai, L.L. Multiagent deep reinforcement learning-based cooperative optimal operation with strong scalability for residential microgrid clusters. *Energy* **2025**, *314*, 134165. [CrossRef]
219. Jin, S.; Wang, S.; Fang, F. Game theoretical analysis on capacity configuration for microgrid based on multi-agent system. *Int. J. Electr. Power Energy Syst.* **2021**, *125*, 106485. [CrossRef]
220. Tan, B.; Chen, H.; Zheng, X.; Huang, J. Two-stage robust optimization dispatch for multiple microgrids with electric vehicle loads based on a novel data-driven uncertainty set. *Int. J. Electr. Power Energy Syst.* **2022**, *134*, 107359. [CrossRef]
221. Jani, A.; Karimi, H.; Jadid, S. Two-layer stochastic day-ahead and real-time energy management of networked microgrids considering integration of renewable energy resources. *Appl. Energy* **2022**, *323*, 119630. [CrossRef]
222. Ning, L.; Liang, K.; Zhang, B.; Li, G. A two-layer optimal scheduling method for multi-energy virtual power plant with source-load synergy. *Energy Rep.* **2023**, *10*, 4751–4760. [CrossRef]
223. Hou, J.; Yu, W.; Xu, Z.; Ge, Q.; Li, Z.; Meng, Y. Multi-time scale optimization scheduling of microgrid considering source and load uncertainty. *Electr. Power Syst. Res.* **2023**, *216*, 109037. [CrossRef]
224. Zheng, X.; Bai, F.; Jin, T. Assessing customer-side demand response identification for optimal scheduling considering satisfaction level for microgrids. *Int. J. Electr. Power Energy Syst.* **2025**, *164*, 110368. [CrossRef]
225. Sun, Y.; Wang, X.; Gao, L.; Yang, H.; Zhang, K.; Ji, B.; Zhang, H. Multi-objective optimal scheduling for microgrids-improved goose algorithm. *Energies* **2024**, *17*, 6376. [CrossRef]
226. Freire Barceló, T.; Martín Martínez, F.; Sánchez Miralles, Á. Demand response cost analysis and its effect on system planning. *Int. J. Electr. Power Energy Syst.* **2025**, *165*, 110483. [CrossRef]
227. Hu, D.; Fan, Y.; Shao, W. Optimal sizing and operation of microgrid considering renewable energy uncertainty based on scenario generation. *J. Energy Storage* **2025**, *109*, 115174. [CrossRef]
228. Mehleri, E.D.; Sarimveis, H.; Markatos, N.C.; Papageorgiou, L.G. Optimal design and operation of distributed energy systems: Application to Greek residential sector. *Renew. Energy* **2013**, *51*, 331–342. [CrossRef]

229. Alamir, N.; Kamel, S.; Abdelkader, S.M. Stochastic multi-layer optimization for cooperative multi-microgrid systems with hydrogen storage and demand response. *Int. J. Hydrogen Energy* **2025**, *100*, 688–703. [CrossRef]
230. Chen, H.; Yang, S.; Chen, J.; Wang, X.; Li, Y.; Shui, S.; Yu, H. Low-carbon environment-friendly economic optimal scheduling of multi-energy microgrid with integrated demand response considering waste heat utilization. *J. Clean. Prod.* **2024**, *450*, 141415. [CrossRef]
231. Wang, C.; Li, X. Optimization scheduling of microgrid comprehensive demand response load considering user satisfaction. *Sci. Rep.* **2024**, *14*, 16034. [CrossRef]
232. Zhou, S.; Yan, R.; Zhang, J.; He, Y.; Geng, X.; Li, Y.; Yu, C. Optimizing interaction in renewable-vehicle-microgrid systems: Balancing battery health, user satisfaction, and participation. *Renew. Energy* **2025**, *245*, 122823. [CrossRef]
233. Chen, H.; Gao, L.; Zhang, Z. Multi-objective optimal scheduling of a microgrid with uncertainties of renewable power generation considering user satisfaction. *Int. J. Electr. Power Energy Syst.* **2021**, *131*, 107142. [CrossRef]
234. Chen, J.J.; Qi, B.X.; Rong, Z.K.; Peng, K.; Zhao, Y.L.; Zhang, X.H. Multi-energy coordinated microgrid scheduling with integrated demand response for flexibility improvement. *Energy* **2021**, *217*, 119387. [CrossRef]
235. Wu, Y.; Hu, M.; Liao, M.; Liu, F.; Xu, C. Risk assessment of renewable energy-based island microgrid using the HFLTS-cloud model method. *J. Clean. Prod.* **2021**, *284*, 125362. [CrossRef]
236. Isfakul Anam, M.; Nguyen, T.-T.; Vu, T. Risk-based preventive energy management for resilient microgrids. *Int. J. Electr. Power Energy Syst.* **2023**, *154*, 109391. [CrossRef]
237. Liu, H.; Tang, W. Multi-objective bi-level programs for optimal microgrid planning considering actual BESS lifetime based on WGAN-GP and info-gap decision theory. *J. Energy Storage* **2024**, *89*, 111510. [CrossRef]
238. Abid, M.d.S.; Apon, H.J.; Hossain, S.; Ahmed, A.; Ahshan, R.; Lipu, M.S.H. A novel multi-objective optimization based multi-agent deep reinforcement learning approach for microgrid resources planning. *Appl. Energy* **2024**, *353*, 122029. [CrossRef]
239. Kharrich, M.; Mohammed, O.H.; Alshammari, N.; Akherraz, M. Multi-objective optimization and the effect of the economic factors on the design of the microgrid hybrid system. *Sustain. Cities Soc.* **2021**, *65*, 102646. [CrossRef]
240. Wen, Y.; Fan, P.; Hu, J.; Ke, S.; Wu, F.; Zhu, X. An optimal scheduling strategy of a microgrid with V_2G based on deep Q-Learning. *Sustainability* **2022**, *14*, 10351. [CrossRef]
241. San, G.; Zhang, W.; Guo, X.; Hua, C.; Xin, H.; Blaabjerg, F. Large-disturbance stability for power-converter-dominated microgrid: A review. *Renew. Sustain. Energy Rev.* **2020**, *127*, 109859. [CrossRef]
242. Wang, R.; Hsu, S.-C.; Zheng, S.; Chen, J.-H.; Li, X.I. Renewable energy microgrids: Economic evaluation and decision making for government policies to contribute to affordable and clean energy. *Appl. Energy* **2020**, *274*, 115287. [CrossRef]
243. Hirsch, A.; Parag, Y.; Guerrero, J. Microgrids: A review of technologies, key drivers, and outstanding issues. *Renew. Sustain. Energy Rev.* **2018**, *90*, 402–411. [CrossRef]
244. Mariam, L.; Basu, M.; Conlon, M.F. Microgrid: Architecture, policy and future trends. *Renew. Sustain. Energy Rev.* **2016**, *64*, 477–489. [CrossRef]
245. Olabi, A.G.; Onumaegbu, C.; Wilberforce, T.; Ramadan, M.; Abdelkareem, M.A.; Al-Alami, A.H. Critical review of energy storage systems. *Energy* **2021**, *214*, 118987. [CrossRef]
246. Aneke, M.; Wang, M. Energy storage technologies and real life applications—A state of the art review. *Appl. Energy* **2016**, *179*, 350–377. [CrossRef]
247. Amir, M.; Deshmukh, R.G.; Khalid, H.M.; Said, Z.; Raza, A.; Muyeen, S.; Nizami, A.-S.; Elavarasan, R.M.; Saidur, R.; Sopian, K. Energy storage technologies: An integrated survey of developments, global economical/environmental effects, optimal scheduling model, and sustainable adaption policies. *J. Energy Storage* **2023**, *72*, 108694. [CrossRef]
248. Danehkar, S.; Yousefi, H. A comprehensive overview on water-based energy storage systems for solar applications. *Energy Rep.* **2022**, *8*, 8777–8797. [CrossRef]
249. Koohi-Fayegh, S.; Rosen, M.A. A review of energy storage types, applications and recent developments. *J. Energy Storage* **2020**, *27*, 101047. [CrossRef]
250. Frate, G.F.; Ferrari, L.; Desideri, U. Energy storage for grid-scale applications: Technology review and economic feasibility analysis. *Renew. Energy* **2021**, *163*, 1754–1772. [CrossRef]
251. Mabrouk, R.; Naji, H.; Benim, A.C.; Dhahri, H. A state of the art review on sensible and latent heat thermal energy storage processes in porous media: Mesoscopic Simulation. *Appl. Sci.* **2022**, *12*, 6995. [CrossRef]
252. Qiao, J.; Mi, Y.; Shen, J.; Lu, C.; Cai, P.; Ma, S.; Wang, P. Optimization schedule strategy of active distribution network based on microgrid group and shared energy storage. *Appl. Energy* **2025**, *377*, 124681. [CrossRef]
253. Dai, B.; Wang, H.; Li, B.; Li, C.; Tan, Z. Capacity model and optimal scheduling strategy of multi-microgrid based on shared energy storage. *Energy* **2024**, *306*, 132472. [CrossRef]
254. Fang, Y.; Yang, J.; Jiang, W. Optimal scheduling strategy of microgrid based on reactive power compensation of electric vehicles. *Energies* **2023**, *16*, 7507. [CrossRef]

255. Xiao, G.; Zhang, M.; Huang, W.; Mo, Z.; Xie, H.; Tang, X. A data-driven hybrid robust optimization approach for microgrid operators in the energy reserve market considering different wind power producers' strategies. *Appl. Energy* **2025**, *386*, 125564. [CrossRef]
256. Huang, W.; Luo, K.; Li, Y.; Liu, H.; Qiang, J. Multi-objective planning of community microgrid based on electric vehicles' orderly charging/discharging strategy. *J. Energy Storage* **2025**, *114*, 115623. [CrossRef]
257. Salyani, P.; Zare, K.; Javani, N.; Boynuegri, A.R. Risk-based scheduling of multi-energy microgrids with Power-to-X technology under a multi-objective framework. *Sustain. Cities Soc.* **2025**, *122*, 106245. [CrossRef]
258. Qiao, J.; Mi, Y.; Ma, S.; Han, Y.; Wang, P. Trilayer stackelberg game scheduling of active distribution network based on microgrid group leasing shared energy storage. *Appl. Energy* **2025**, *382*, 125157. [CrossRef]
259. Rochd, A.; Raihani, A.; Mahir, O.; Kissaoui, M.; Laamim, M.; Lahmer, A.; El-Barkouki, B.; El-Qasery, M.; Sun, H.; Guerrero, J.M. Swarm intelligence-driven multi-objective optimization for microgrid energy management and trading considering DERs and EVs integration: Case studies from green energy Park, Morocco. *Results Eng.* **2025**, *25*, 104400. [CrossRef]
260. Zhao, Z.; Xu, J.; Lei, Y.; Liu, C.; Shi, X.; Lai, L.L. Robust dynamic dispatch strategy for multi-uncertainties integrated energy microgrids based on enhanced hierarchical model predictive control. *Appl. Energy* **2025**, *381*, 125141. [CrossRef]
261. Li, L.L.; Ji, B.X.; Li, Z.T.; Lim, M.K.; Sethanan, K.; Tseng, M.L. Microgrid energy management system with degradation cost and carbon trading mechanism: A multi-objective artificial hummingbird algorithm. *Appl. Energy* **2025**, *378*, 124853. [CrossRef]
262. Yang, M.; Wang, J.; Cao, X.; Gu, D. Economic dispatch of microgrid generation-load-storage based on dynamic bi-level game of multiple stakeholders. *Energy* **2024**, *313*, 133931. [CrossRef]
263. Hussain, J.; Huang, Q.; Li, J.; Hussain, F.; Mirjat, B.A.; Zhang, Z.; Ahmed, S.A. A fully decentralized demand response and prosumer peer-to-peer trading for secure and efficient energy management of community microgrid. *Energy* **2024**, *312*, 133538. [CrossRef]
264. Singh, U.; Singh, S.; Gupta, S.; Alotaibi, M.A.; Malik, H. Forecasting rooftop photovoltaic solar power using machine learning techniques. *Energy Rep.* **2025**, *13*, 3616–3630. [CrossRef]
265. Ani, A.; Khor, E.T. Development and evaluation of predictive models for predicting students performance in MOOCs. *Educ. Inf. Technol* **2024**, 13905–13928. [CrossRef]
266. Nijat, M.; David, E.; Peter, F.; Peter, L. Evaluating forecasting methods by considering different accuracy measures. *Procedia Comput. Sci.* **2016**, *95*, 264–271. [CrossRef]

Disclaimer/Publisher's Note: The statements, opinions and data contained in all publications are solely those of the individual author(s) and contributor(s) and not of MDPI and/or the editor(s). MDPI and/or the editor(s) disclaim responsibility for any injury to people or property resulting from any ideas, methods, instructions or products referred to in the content.